

# MOLECULAR SPECTROSCOPY : MODERN RESEARCH

VOLUME II

*Edited by*

*K. NARAHARI RAO*

DEPARTMENT OF PHYSICS  
THE OHIO STATE UNIVERSITY  
COLUMBUS, OHIO

1976



ACADEMIC PRESS      New York   San Francisco   London  
A SUBSIDIARY OF HAROURT BRACE JOVANOVICH, PUBLISHERS

7, 1605 (1964).  
Polyakov, *Radiofiz. U.S.S.R.* **12**,

).  
*Instrum.* **34**, 843 (1963).

9 (1974).

ys. **62**, 1040 (1975).  
*hem. Phys.* **62**, 4796 (1975).  
*hem. Phys.* **63**, 2724 (1975).

Holland Publ., Amsterdam, 1967.  
tern Research" (K. N. Rao and

9).  
*strum.* **30**, 765 (1959).

sk. *Untersuchungen an Mol. III*,

*Jol. Spectrosc.*, Tours paper Q1

nnier, and M. L. Deutsch, *Phys.*

nnewisser, *Symp. Mol. Structure*

. *Phys.* **49**, 3465 (1968).  
*Int. Rev. Sci.* **1** (1972).  
atum Chemistry and Molecular

9a, 633 (1974).

*Jol. Spectrosc.* **56**, 449 (1975).

## 2.2 New Methods in Submillimeter Microwave Spectroscopy

*A. F. Krupnov and A. V. Burenin*

*Radiophysical Research Institute  
Gorkii, USSR*

### Introduction

Traditional methods of submillimeter microwave spectroscopy are based on the use of harmonic generators and microwave radiation detectors [1-4]. Recently new methods have been developed using broadband submillimeter backward wave oscillators (BWO's) and acoustic detection of the signal from spectral lines by the gas itself (the first paper [5] dates back to the year 1970, successive stages of development are given in references [6-8]). By employing a spectrometer equipped with a BWO and an acoustic detector (which we call RAD, from the Russian phrase "radiospectroscope with acoustic detector"), it has been possible to achieve an increase in the submillimeter spectrometer sensitivity of several orders of magnitude, to observe for the first time continuous microwave spectra up to frequencies exceeding 1 THz ( $1 \text{ THz} = 10^{12} \text{ Hz}$ ), and to make effective use of large radiation powers, etc. These results stimulated a more thorough analysis of microwave spectrometer sensitivity limits and practical ways for their realization, as well as a consideration of new possibilities of investigations and the development of mathematical apparatus suitable for processing broad continuous spectral records containing hundreds and thousands of lines. This review gives the first account of the results of submillimeter microwave spectroscopy development in this direction.

### 1. Principles and Sensitivity Limits of Microwave Spectrometers

#### 1.1. SPECTROMETER CLASSIFICATION

All existing spectrometers may be divided into two main classes (Fig. 1) according to two methods of obtaining the signal from the spectral lines of the sample investigated. The first method involves registering the change in

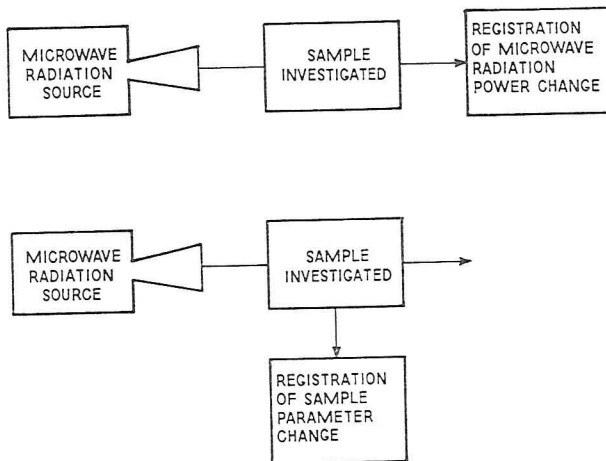


FIG. 1. Two main classes of spectrometers (classification according to the method of signal formation from the spectral lines).

microwave radiation power after passage through the sample; the second involves registering the change in one or more sample parameters under the action of the radiation [9, 10]. Considering the region of spectrometer operation close to the sensitivity limit, one may assume that the fraction of power absorbed by the sample  $P_s$  is small, i.e.,  $P_s \ll P_0$ , where  $P_0$  is the microwave radiation source power. Thus, in the first class of spectrometers the useful signal  $P_s$  must be observed in the presence of a large (noninformative) background  $P_0$ , and this is the main source of sensitivity-decreasing phenomena (including the increase of noise, appearance of false signals, etc.) [2]. The microwave spectrometers commonly used are devices of the first class and the above circumstances limit their absorption coefficient sensitivity to a value of the order of  $10^{-10} \text{ cm}^{-1}$  at a time constant of 1 sec, and limit the allowed power to a value of  $10^{-3} \text{ W}$  [2]. Spectrometers of the second class look more promising since the null signal detection principle for the microwave power is intrinsic to them, and only the useful signal  $P_s$  is registered. The detector noise in the absence of spectral lines does not depend on the radiation power passing through the sample and the absorption coefficient sensitivity increases at a rate proportional to the radiation power up to power levels causing transition saturation or breakdown in the gas. The absence of detector reaction outside the spectral lines also eliminates false signals. As a result, the absorption coefficient sensitivity of microwave spectrometers of the second class (when powerful enough radiation sources are used) may significantly exceed the aforementioned figure of  $10^{-10} \text{ cm}^{-1}$  at a time constant of 1 sec. Numerical estimates are given below.

## 1.2. SENSIVITY LIMI

We take the lim related resolving pc fluctuation processe sufficient for some

Here  $|\mu_{ij}|^2$  and  $\Delta$  moment and the hc transition, respectiv

( $n$  is the population frequency) and the microwave power.

A. The primary radiation at the lin resonance levels in selective detector o i.e., a device of the fulfilled and the pi then naturally in th ate particles in the l equilibrium sum pc the transition is eq

where  $t$  is the cou counted  $\sim N_{12} \Delta v$  molecular beam scheme: "beam sou field inducing tran: For gas microwave

B. The seconda ent resonance radi parameters. For re acoustic detectors) When the modulat modulation frequ to  $\Delta E_s \sim P_s \tau^{cell}$  (u is the characteristic characteristic time

IN  
REGISTRATION  
OF MICROWAVE  
RADIATION  
POWER CHANGE

## 1.2. SENSIVITY LIMITS

We take the limiting factor in estimates of the sensitivity (and closely related resolving power) of spectrometers of the second class to be thermal fluctuation processes in the gas. The radiation source power is assumed to be sufficient for some saturation of the transition, i.e.,

$$P_0 \sim h^2(\Delta\nu)^2cS/8\pi|\mu_{ij}|^2. \quad (1)$$

Here  $|\mu_{ij}|^2$  and  $\Delta\nu$  are the square of the matrix element of the dipole moment and the homogeneous (collisional in this case) line half-width of the transition, respectively, and  $S$  is the cell cross section area. Then

$$P_s \sim nhv\Delta\nu \quad (2)$$

( $n$  is the population difference between the levels involved,  $v$  is the transition frequency) and there are no signal losses produced because of insufficient microwave power.

A. The primary effect which occurs in a gas under the action of coherent radiation at the line frequency is the change of the particle number in the resonance levels in comparison with the initial Boltzmann distribution. A selective detector of this effect might be a "counter of particles in the level," i.e., a device of the quantum counter type [11]. If we assume that Eq. (1) is fulfilled and the process of counting does not introduce additional noise, then naturally in this case the maximum sensitivity is achieved, since separate particles in the level may be counted. It is easy to show that the threshold equilibrium sum population of the resonance levels necessary for registering the transition is equal to

$$N_{12} \sim (1/\Delta\nu t)[1 + \exp(-hv/kT)]^2, \quad (3)$$

where  $t$  is the counting time (it is assumed that the mean particle number counted  $\sim N_{12}\Delta\nu t \gg 1$ ). Maximally close to this case (in principle) is a molecular beam microwave spectrometer operating according to the scheme: "beam source  $\rightarrow$  state separator as polarizer  $\rightarrow$  region of microwave field inducing transitions  $\rightarrow$  state separator as analyzer  $\rightarrow$  particle counter." For gas microwave spectroscopy, such counters are generally absent.

B. The secondary effect which occurs in a gas under the action of coherent resonance radiation is the change of macroscopic thermodynamic gas parameters. For registering this effect there now exist detectors (for example, acoustic detectors), the sensitivity of which may reach the thermal limit. When the modulated radiation is absorbed, the gas changes its energy at the modulation frequency. The maximum amplitude of these variations is equal to  $\Delta E_s \sim P_s \tau^{cell}$  (under the condition that  $\tau^{cell} \sim \tau^{mod}$ , where  $\tau^{cell} \sim 1/\Delta\omega^{cell}$  is the characteristic time of thermal gas relaxation in the cell, and  $\tau^{mod}$  is the characteristic time of modulation). The condition for detecting this effect

against a background of the gas energy fluctuations (and hence the effect of any thermodynamic parameter variation) is written as

$$\Delta E_s \sim [\bar{E}_\omega^2 \Delta\omega^{rec}]^{1/2}, \quad (4)$$

where  $\bar{E}_\omega^2$  is the spectral density of the power fluctuations of the gas energy close to the modulation frequency,  $\Delta\omega^{rec}$  is the receiver bandwidth. In order of magnitude,  $\bar{E}_\omega^2 \Delta\omega^{cell} \sim (kT)^2 N$ , where  $N$  and  $T$  are the total gas particle number in the cell and the gas temperature. For the minimum detectable value of  $n$  one obtains

$$n_{min} \sim (kT/h\nu \Delta\nu)(N \Delta\omega^{cell} \Delta\omega^{rec})^{1/2}. \quad (5)$$

The appearance of the quantity  $N^{1/2}$  on the right-hand side of the equation is associated with the observation of the useful signal in the presence of a background of fluctuation processes in the gas, the number of degrees of freedom which is proportional to  $N$ . The sensitivity to the parameter  $n_{min}$  increases with increasing homogeneous linewidth, since the threshold of the line saturation shifts and at the same time the resolving power  $\nu/\Delta\nu$  drops. Actually, this is a demonstration of the "pure" connection between the sensitivity and the resolving power of the microwave spectrometer. Introducing the parameter  $n_{min} \Delta\nu/\nu$  one obtains

$$n_{min} \Delta\nu/\nu \sim (kT/h\nu^2)(N \Delta\omega^{cell} \Delta\omega^{rec})^{1/2}. \quad (6)$$

From Eqs. (5) and (6) it is seen that an increase in the spectrometer operating frequency is advantageous from the point of view of improvement of the

TABLE I  
Sensitivity Limits of Microwave Spectrometers

$ \mu_{ij} $ (debyes)	$\Delta\nu$ (MHz)	Parameters	$10^{+0}$	$10^{-1}$	$10^{+2}$	$10^{+3}$
$10^{-0}$	$10^{-0}$	$n_{min}$	$10^{+5}$	$10^{-4}$	$10^{+3}$	$10^{+2}$
		$\gamma_{min}$ ( $\text{cm}^{-1}$ )	$10^{-9}$	$10^{-11}$	$10^{-13}$	$10^{-15}$
		$\gamma_{min}(\Delta\nu/\nu)$ ( $\text{cm}^{-1}$ )	$2 \cdot 10^{-15}$	$2 \cdot 10^{-16}$	$2 \cdot 10^{-17}$	$2 \cdot 10^{-18}$
		$P_0$ (W)	$5 \cdot 10^{-3}$	$5 \cdot 10^{-1}$	$5 \cdot 10^{+1}$	$5 \cdot 10^{+3}$
$10^{-1}$	$10^{-1}$	$n_{min}$	$10^{+5}$	$10^{-4}$	$10^{+3}$	$10^{+2}$
		$\gamma_{min}$ ( $\text{cm}^{-1}$ )	$10^{-11}$	$10^{-13}$	$10^{-15}$	$10^{-17}$
		$\gamma_{min}(\Delta\nu/\nu)$ ( $\text{cm}^{-1}$ )	$2 \cdot 10^{-17}$	$2 \cdot 10^{-18}$	$2 \cdot 10^{-19}$	$2 \cdot 10^{-20}$
		$P_0$ (W)	$5 \cdot 10^{-1}$	$5 \cdot 10^{+1}$	$5 \cdot 10^{+3}$	$5 \cdot 10^{+5}$
$10^{-2}$	$10^{-2}$	$n_{min}$	$10^{+5}$	$10^{-4}$	$10^{+3}$	$10^{+2}$
		$\gamma_{min}$ ( $\text{cm}^{-1}$ )	$10^{-13}$	$10^{-15}$	$10^{-17}$	$10^{-19}$
		$\gamma_{min}(\Delta\nu/\nu)$ ( $\text{cm}^{-1}$ )	$2 \cdot 10^{-19}$	$2 \cdot 10^{-20}$	$2 \cdot 10^{-21}$	$2 \cdot 10^{-22}$
		$P_0$ (W)	$5 \cdot 10^{+1}$	$5 \cdot 10^{+3}$	$5 \cdot 10^{+5}$	$5 \cdot 10^{+7}$

## 2.2 NEW METHODS

limiting parameters. The sensitivity coefficient sensitivity estimates of these parameters are proportional to  $P_0$  for  $\Delta\omega^{rec} = 1 \text{ sec}^{-1}$ ,  $N = n_{min} \Delta\nu/\nu$  is then fixed. Conclusion concerning the microwave spectrometer.

### 2. Submillimeter Sources and the Acoustic

#### 2.1. GENERAL DESCRIPTION

In the RAD (Fig. 2) the source—the source—placed cells containing the mixer-multiplier of the system. When the radiation of the spectral line the gas increase in the cell. The source is modulated with an a component of the gas pressure signal from the absorption placed in the cell. After recorded. The BWO approximately an oct spectrum of the gas. It is in references [13, 14]. by the reference radiations measured by a counter are used. According to the second (B) class of spectra from the line. This leads to a levity increase) to the following high power radiation new perspectives in the signal detection provide frequency and the absorption conjunction with elect

† Gas sounding when air was used in the nineteenth century [12].

ns (and hence the effect of  $\gamma_{\min}$ ) as

$$(4)$$

situations of the gas energy receiver bandwidth. In order  $\Gamma$  are the total gas particle  $n$  the minimum detectable

$$(5)$$

-hand side of the equation signal in the presence of a the number of degrees of  $\gamma_{\min}$  to the parameter  $n_{\min}$  since the threshold of the solving power  $v/\Delta v$  drops. connection between the wave spectrometer. Intro-

$$(6)$$

the spectrometer operation view of improvement of the

ometers

limiting parameters. One may obtain analogous expressions for the absorption coefficient sensitivity  $\gamma_{\min}$  and  $\gamma_{\min} \Delta v/v$  [10]. Table I gives numerical estimates of these parameters for different  $\Delta v$  and  $|\mu_{ij}|$ , and the corresponding power  $P_0$  for  $T = 300^\circ\text{K}$ ,  $v = 500 \text{ GHz}$ ,  $\Delta\omega^{\text{cell}} = 10^3 \text{ sec}^{-1}$ ,  $\Delta\omega^{\text{rec}} = 1 \text{ sec}^{-1}$ ,  $N = 10^{17}$ ,  $l = 10 \text{ cm}$ , and  $S = 1 \text{ cm}^2$ . The parameter  $n_{\min} \Delta v/v$  is then fixed and equal to  $2 \times 10^{-1}$ . The estimates confirm the conclusion concerning the possibility of a considerable increase in the microwave spectrometer sensitivity in comparison with the existing level.

## 2. Submillimeter Spectrometer with a BWO and the Acoustic Detector (RAD)

### 2.1. GENERAL DESCRIPTION

In the RAD (Fig. 2) the radiation of the primary monochromatic submillimeter source—the BWO—passes through one or several successively placed cells containing the gases investigated and is then directed to the mixer-multiplier of the BWO stabilization and frequency measurement system. When the radiation frequency coincides with the frequency of the spectral line the gas absorbs the power, heats, and produces a pressure increase in the cell.<sup>†</sup> The amplitude or frequency of the BWO radiation is modulated with an audio range modulation frequency. The spectral component of the gas pressure variations at the modulation frequency is the signal from the absorption line registered by the sensitive microphone placed in the cell. After amplification and synchronous detection the signal is recorded. The BWO radiation frequency may be scanned electronically by approximately an octave, which permits making a record of the absorption spectrum of the gas. Descriptive data for the 70–1500 GHz BWO's are given in references [13, 14]. Up to 500 GHz the BWO frequency may be controlled by the reference radio frequency oscillator; the frequency of the latter is measured by a counter. In the higher frequency region, nonstabilized BWO's are used. According to the classification in Section 1, the RAD belongs to the second (B) class of spectrometers because of the manner of signal formation from the line. This leads (besides the aforementioned possibility of a sensitivity increase) to the following properties important in practice: (i) the use of high power radiation sources without an increase in receiver noise opens new perspectives in nonlinear spectroscopy; (ii) the thermal volume “null” signal detection provides independence of the sensitivity on the radiation frequency and the absence of false signals from interference effects, which in conjunction with electronic control of the BWO frequency permits carrying

<sup>†</sup> Gas sounding when absorbing modulated radiation was discovered in the latter part of the nineteenth century [12].

	$10^{+2}$	$10^{+3}$
4	$10^{+3}$	$10^{+2}$
11	$10^{-13}$	$10^{-15}$
16	$2 \cdot 10^{-17}$	$2 \cdot 10^{-18}$
1	$5 \cdot 10^{+1}$	$5 \cdot 10^{+3}$
4	$10^{+3}$	$10^{+2}$
13	$10^{-15}$	$10^{-17}$
18	$2 \cdot 10^{-19}$	$2 \cdot 10^{-20}$
1	$5 \cdot 10^{+3}$	$5 \cdot 10^{+5}$
4	$10^{+3}$	$10^{+2}$
15	$10^{-17}$	$10^{-19}$
20	$2 \cdot 10^{-21}$	$2 \cdot 10^{-22}$
3	$5 \cdot 10^{+5}$	$5 \cdot 10^{+7}$

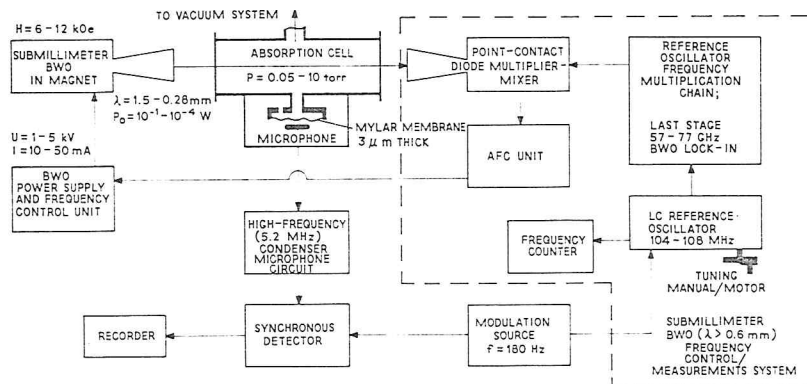


FIG. 2. Submillimeter RAD spectrometer. The main parts are the submillimeter BWO, two absorption cells with acoustic receivers (only one cell is shown), and the system of BWO frequency control and measurement.

out automatic records of broad parts of the spectrum; (iii) the signal formation (for the majority of spectral lines) from a small fraction of the radiation power passing through the cell permits making simultaneous independent records of several gas spectra in several absorption cells with microphones, and the utilization of the full radiation power passing through the cells in the system for stabilization and measurement of the BWO frequency. The main parts of the RAD spectrometer are described below. The characteristics obtained are illustrated by the spectra in Figs. 3-6, 12, and 18.

FIG. 4. Broadband rec...  
are shown).

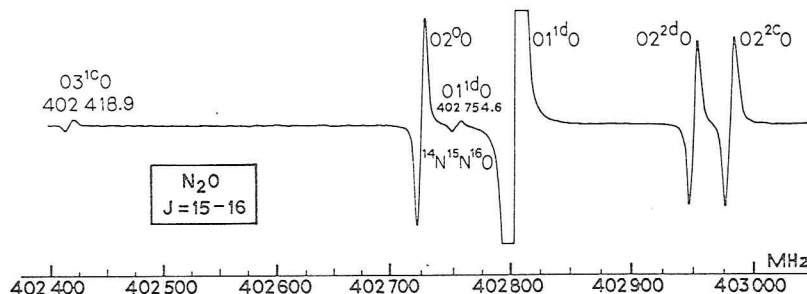
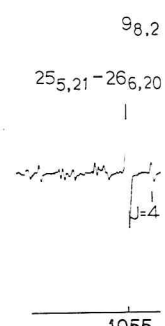
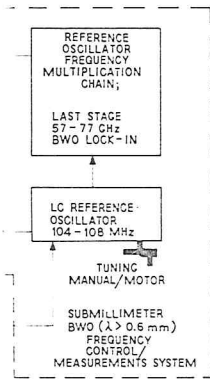


FIG. 3. The record of vibrational satellites of the rotational transition  $J = 15-16$  in  $^{14}\text{N}^{14}\text{N}^{16}\text{O}$  and in  $^{14}\text{N}^{15}\text{N}^{16}\text{O}$  in natural abundance at the highest sensitivity presently achievable in the submillimeter band, i.e.,  $6 \times 10^{-9} \text{ cm}^{-1}$ . Lines are recorded in the form of the first derivative of the absorption profile. The measured frequencies of satellites  $^{14}\text{N}^{14}\text{N}^{16}\text{O}$  ( $03^1\text{C}0$ ) and  $^{14}\text{N}^{15}\text{N}^{16}\text{O}$  ( $01^1\text{d}0$ ) are given in the figure.

FIG. 5. The first rec...  
Lines are recorded in th...





the submillimeter BWO, two and the system of BWO

(iii) the signal formation of the radiation instantaneous independent cells with microphones, through the cells in the frequency. The main. The characteristics 1. and 18.

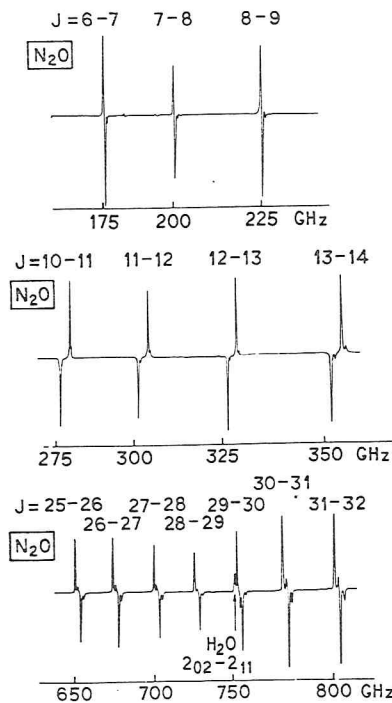
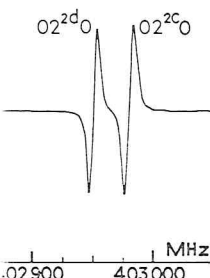


FIG. 4. Broadband record of the rotational  $\text{N}_2\text{O}$  spectrum (only three parts of the spectrum are shown).



transition  $J = 15-16$  in highest sensitivity presently recorded in the form of the of satellites  $^{14}\text{N}^{14}\text{N}^{16}\text{O}$

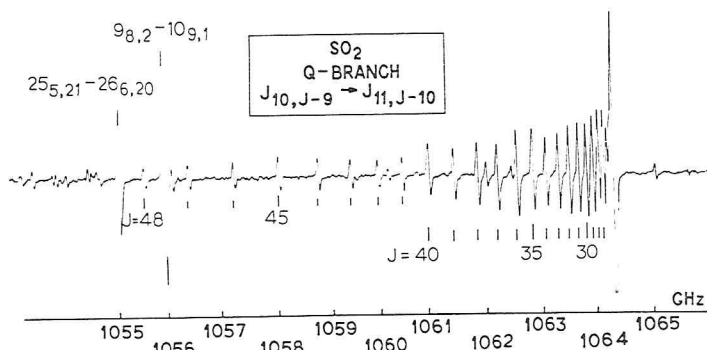


FIG. 5. The first record of a microwave spectrum at frequencies above 1 THz ( $10^{12} \text{ Hz}$ ). Lines are recorded in the form of the first derivative of the absorption profile.

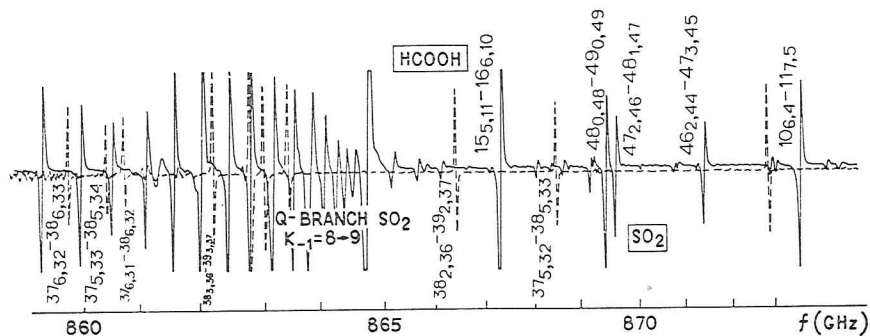


FIG. 6. A part of a simultaneous record of two submillimeter spectra: the reference  $\text{SO}_2$  spectrum (—) and the investigated  $\text{HCOOH}$  spectrum (---). Lines are recorded in the form of the first derivatives of the absorption profiles. Such records may cover regions of hundreds of gigahertz and may be used for the initial analysis of the spectra investigated.

## 2.2. CELL AND DETECTOR (RECEIVER)

The gas cell, microphone, and electronic detector circuit (Fig. 7) must provide the maximum signal-to-noise ratio for weak lines ( $\gamma l \ll 1$ ) for given resolving power of the spectrometer and radiation power passing through the cell.

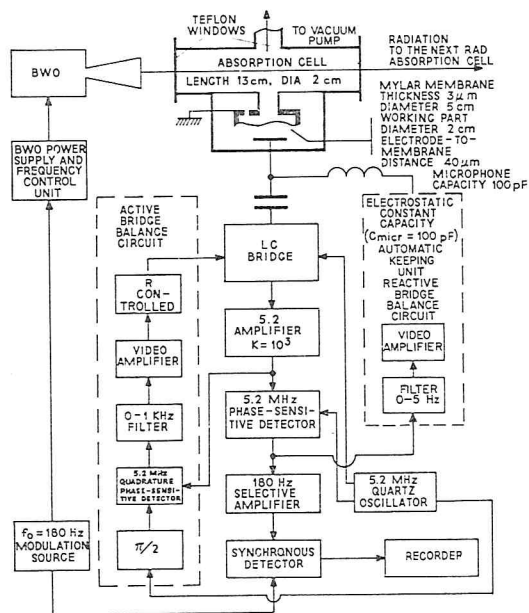


FIG. 7. RAD absorption cell and microphone receiver circuit.

The conditions for 1 microphone placed in

Equation (7) connect constant of the therm gas pressure variation cities and provides th tions into membrane volume,  $R$  and  $T^*$  are the force per unit ed. the expression for the ing conclusions [15] signal increases slow mun modulation freq operating pressure is power of the spectr the smallest (transve parameters the signa to a value defined b signal strength is sat and (8) on the gas p pressure.

The realization of the most difficult pr used (a membrane i proportionally to  $m$ . is very desirable fro the electronics circu

The spectrometer the microphone me motion of the mem inherent noise of the trometer is obtained defined preferably t ameters are practice similarly transforme dence on the cell le

<sup>†</sup> Calculations are ma initial tension and the fre than the modulation fre

The conditions for maximum condenser microphone output signal by the microphone placed in the cell are [15]:

$$\omega_M \tau^{\text{cell}} \simeq 1 \quad (7)$$

$$m = \pi p R^4 / 8 V T^* \simeq 1. \quad (8)$$

Equation (7) connects the angular modulation frequency  $\omega_M$  and the time constant of the thermal processes  $\tau^{\text{cell}}$ , and provides maximum amplitude of gas pressure variations. Equation (8) connects the gas and membrane elasticities and provides the most effective transformation of the pressure variations into membrane displacements.<sup>†</sup> Here  $p$  is the gas pressure,  $V$  is the cell volume,  $R$  and  $T^*$  are the radius and initial tension of the membrane ( $T^*$  is the force per unit edge length). Analysis of these matching conditions and the expression for the signal strength obtained in this case permit the following conclusions [15]: (i) when the matching conditions are fulfilled, the signal increases slowly with decreasing modulation frequency. The minimum modulation frequency is then defined by environmental noise. (ii) The operating pressure is sufficiently strictly defined by the desired resolving power of the spectrometer. Hence from Eq. (7) we obtain the value of the smallest (transverse) dimension of the cell. (iii) For given membrane parameters the signal strength increases with increasing cell length only up to a value defined by Eq. (8). Upon further increasing the cell length, the signal strength is saturated. (iv) The dependence of the matching Eqs. (7) and (8) on the gas pressure leads to a dependence of the output signal on pressure.

The realization of the matching condition  $m \simeq 1$  at small gas pressures is the most difficult problem in practice, even when rather thin membranes are used (a membrane is stiffer than gas,  $m \ll 1$ ). In this case the signal drops proportionally to  $m$ . The maximum close approach to fulfillment of Eq. (8) is very desirable from the point of view of requirements for the sensitivity of the electronics circuit.

The spectrometer output noise is defined by the thermal fluctuations of the microphone membrane in the gas (both due to inherent Brownian motion of the membrane and to Brownian motion of the gas) and by the inherent noise of the electronics circuit. The limiting sensitivity of the spectrometer is obtained when the thermal fluctuations of the membrane are defined preferably by Brownian motion of the gas. In this case the parameters are practically unrestricted, since the gas noise and the signal are similarly transformed into membrane displacements. Only the weak dependence on the cell length remains. The signal-to-noise ratio increases as  $l^{1/2}$ ,

<sup>†</sup> Calculations are made for the real case in which the membrane elasticity is defined by its initial tension and the frequency of free oscillations of the membrane in vacuum is much greater than the modulation frequency.

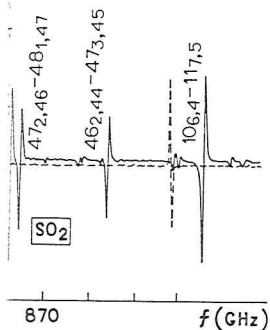
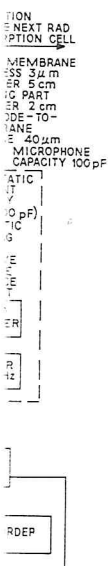


Fig. 7. Spectra: the reference  $\text{SO}_2$  spectra are recorded in the form of cover regions of hundreds of investigated.

circuit (Fig. 7) must have lines ( $\gamma l \ll 1$ ) for given power passing through



receiver circuit.

because the effective volume thermal noise sources do not correlate between each other, but the signal sources do. In the absence of line saturation for  $T = 300^\circ\text{K}$ ,  $l = 10 \text{ cm}$ , an integration time of 1 sec, and a typical gas thermal conductivity, one may obtain the following estimate for the limiting absorption coefficient sensitivity of the RAD [15]:

$$\gamma_{\min}(\text{cm}^{-1}) \simeq 4 \times 10^{-11}/P_0, \quad (9)$$

where  $P_0$  is in watts. An analogous estimate may be obtained more roughly using Eq. (4) and the expression for the signal power  $P_s \simeq \gamma l P_0$ . Let us consider the possibilities of achieving this ultimate sensitivity.

The rms displacement of the center of the membrane due to fluctuations connected with Brownian motion in the gas (at  $\omega_M \tau^{\text{cell}} \simeq 1$ ,  $m \ll 1$ ) in the receiver bandwidth  $\Delta\omega^{\text{rec}}$  near the modulation frequency is equal to

$$\sigma_g \simeq (1/4\pi)(kTm \Delta\omega^{\text{rec}}/T^* \Delta\omega^{\text{cell}})^{1/2}, \quad (10)$$

and that due to the inherent membrane Brownian motion is

$$\sigma_m \simeq (1/\pi)(kT \Delta\omega^{\text{rec}}/2Q_M \Omega T^*)^{1/2}. \quad (11)$$

Here  $\Omega$  and  $Q_M$  are the resonant frequency and quality factor of the membrane as a mechanical oscillator in vacuum. For the parameter values  $Q_M \simeq 5 \times 10^2$ ,  $\Omega \simeq 10^4 \text{ sec}^{-1}$ ,  $m \simeq 10^{-2}$ , and  $\Delta\omega^{\text{rec}} \simeq 10^3 \text{ sec}^{-1}$ , the ratio  $\sigma_g/\sigma_m$  is nearly 2.5 and the order of magnitude of  $\sigma_g$  is  $5 \times 10^{-5} \text{ \AA}$  [15].

The electronic circuit must register these rather small fluctuation displacements of the membrane with very weak tension. When the cell is evacuated and filled with the gas to be investigated, considerable displacements of the membrane may occur. These must not influence the sensitivity of the microphone and circuit in the subsequent operation. The most suitable circuit for fulfilling these conditions is the high-frequency bridge condenser microphone circuit with the microphone capacity included in one resonant bridge arm. It will be shown below that the sensitivity of such a circuit is sufficient for detection of gas fluctuations. The use of an automatic bridge balance along two coordinates (microphone capacity by electrostatic control of the membrane position, the circuit losses by an electrically controlled resistor) provides constant sensitivity of the microphone and the circuit.

When the bridge is fed by a quartz oscillator with a sufficiently pure spectrum, then the noise in the narrow sidebands  $\Delta\omega^{\text{rec}}$  at the frequencies  $\omega_q \pm \omega_M$  is caused only by thermal fluctuations in the resonant bridge arms and the circuit sensitivity is equal to

$$\sigma_c \simeq (1/Q)(8/\pi)^{1/2}(kT \Delta\omega^{\text{rec}}/P_q)^{1/2} d. \quad (12)$$

Here  $\omega_q$  is the quartz oscillator frequency,  $Q$  is the quality factor of the microphone resonant circuit at the frequency  $\omega_q$ ,  $P_q$  is the power dissipated in this circuit,  $d$  is the distance between the membrane and the other elec-

trode of the microconductive layer or value  $P_q$  may be in membrane and el The condition for i

and when the value has

Assuming membra circuit, one may  $\omega_q \geq 10^6 \text{ Hz}$ , which

The relatively spon with the cells c stages for a number etc.). At present, th

(with  $P_0$  in watts), particular, at the 10 mW, the sensit

### 2.3. BWO FREQUE

To use success radiation—the BW the problems of sta solution here would to that used in the sufficient stability. submillimeter BW frequency range up ments is solved in t ing the BWO frequ difficult. At presen (with moderate res selected parts of the 500 GHz are obser measurements util lator. Within the fr ilized BWO's are u

not correlate between  
of line saturation for  
a typical gas thermal  
or the limiting absorp-

(9)

obtained more roughly  
ver  $P_s \approx \gamma l P_0$ . Let us  
nsitivity.

ne due to fluctuations  
 $\omega_{\text{cell}} \approx 1, m \ll 1$ ) in the  
ency is equal to

$\omega^2$ , (10)

otion is

$\omega^2$ , (11)

ty factor of the mem-  
the parameter values  
 $\approx 10^3 \text{ sec}^{-1}$ , the ratio  
is  $5 \times 10^{-5} \text{ Å}$  [15].

l fluctuation displace-  
the cell is evacuated  
displacements of the  
nsitivity of the micro-  
ost suitable circuit for  
ge condenser micro-  
one resonant bridge  
a circuit is sufficient  
matic bridge balance  
ostatic control of the  
controlled resistor)  
e circuit.

h a sufficiently pure  
 $\omega_{\text{rec}}$  at the frequencies  
resonant bridge arms

(12)

quality factor of the  
the power dissipated  
and the other elec-

trode of the microphone. The value  $Q$  is defined by the losses in the thin conductive layer on the membrane and is approximately equal to  $10^2$ . The value  $P_q$  may be increased until the electrostatic attractive force between membrane and electrode is compensated by the membrane tension. The condition for membrane stability loss is

$$d/P_q^{1/2} = (Q/4\pi\omega_q T^*)^{1/2}, \quad (13)$$

and when the value  $d/P_q^{1/2}$  is near the optimal from Eqs. (12) and (13), one has

$$\sigma_c \approx (1/\pi)(2kT \Delta\omega_{\text{rec}}/Q\omega_q T^*)^{1/2}. \quad (14)$$

Assuming membrane fluctuations to predominate over fluctuations of the circuit, one may obtain the condition for  $\omega_q$ . In practice we require  $\omega_q \geq 10^6 \text{ Hz}$ , which is easy to fulfill.

The relatively small dimensions of the RAD absorption cells in comparison with the cells of common microwave spectrometers have some advantages for a number of investigations (free radicals, Stark and Zeeman effects, etc.). At present, the experimentally obtained RAD sensitivity is equal to

$$\gamma_{\min}(\text{cm}^{-1}) \approx 6 \times 10^{-11}/P_0, \quad (15)$$

(with  $P_0$  in watts), which is rather close to the theoretical value in Eq. (9). In particular, at the wavelength 0.75 mm, where the BWO power is near 10 mW, the sensitivity  $6 \times 10^{-9} \text{ cm}^{-1}$  is obtained (Fig. 3).

### 2.3. BWO FREQUENCY CONTROL

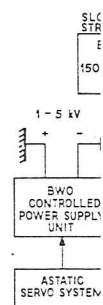
To use successfully the primary sources of coherent submillimeter radiation—the BWO's—for microwave spectroscopy, it is necessary to solve the problems of stabilization and measurement of their frequency. The best solution here would be active digital control of the BWO frequency (similar to that used in the centimeter range [16]) by a tunable reference oscillator of sufficient stability. The possibility of operating systems for phase lock-in submillimeter BWO frequencies was demonstrated in 1970 [17] in the frequency range up to 400 GHz. The problem of BWO frequency measurements is solved in this case automatically. However, the problem of stabilizing the BWO frequency over the whole continuous range is now technically difficult. At present large parts of the submillimeter spectrum are recorded (with moderate resolution) by RAD with a nonstabilized BWO. Then some selected parts of the spectrum (several gigahertz in width) in the range up to 500 GHz are observed with increased resolving power and precise frequency measurements utilizing BWO frequency stabilization by the reference oscillator. Within the frequency range 500–1000 GHz (0.5–1 THz) only nonstabilized BWO's are used now.

Submillimeter BWO's of the type described in reference [13] are two-electrode tubes and control of their frequency is performed by variation of the supply voltage. Variation of the supply voltage from 1 up to 5 kV (at a current of 10 to 50 mA) corresponds to changing the oscillation frequency approximately by a factor of two (by an octave). The frequency dependence on the voltage is nearly 50–100 MHz/V. The use of a highly stable BWO power supply and linear voltage scanning with regulated speed permits continuous spectrum records covering hundreds of gigahertz with a resolution up to  $10^{-5}$  without stabilization by the reference signal (Figs. 4, 5, 18). Frequencies of the spectral lines investigated are determined with an accuracy of  $\sim 5 \times 10^{-5}$  by the use of a simultaneously recorded reference spectrum (in the second cell) (Fig. 6). As a reference spectrum the well known  $\text{SO}_2$ <sup>†</sup> spectrum is used. An accuracy increase up to  $10^{-6}$  may be achieved by measuring the distance between the lines of the reference spectrum and the investigated one by the known method of source frequency modulation [2] (distances can be measured up to 0.5 GHz) with the BWO frequency stabilized at one of the spectral lines [19].

BWO frequency modulation by a square wave and synchronous detection are generally employed for recording the lines. The observed form of the recorded spectral line depends on the relation between the frequency deviation and the spectral line width and varies from the first derivative of the absorption profile (at small deviations) up to two separately recorded lines with opposite signs (at large deviations). The situation here is similar to that in a Stark spectrometer and the requirements for the form of the square-wave modulation are defined by the same conditions as the requirements for the form of the Stark voltage in a Stark spectrometer.

With the BWO frequency stabilized by the reference signal (obtained by frequency multiplication of the reference radio frequency oscillator) the resolving power and the accuracy of the line frequency measurements of the RAD are significantly better. The RAD scheme with the system of frequency stabilization is shown in Fig. 2. The reference oscillator, the frequency of which is measured by the counter, operates in the 100 MHz range. The frequency multiplication chain and the mixer-multiplier of the last stage of the stabilization circuit are similar to those used earlier [20, 21]. The last stage of the frequency multiplication chain consists of the lock-in BWO in the 70 GHz range and the point contact diode at which the multiplication of the 70 GHz BWO frequency and the mixing of harmonics of 70 GHz with the fundamental frequency of the submillimeter BWO occur. The main problems in stabilization of the submillimeter BWO frequency (after obtaining beats with a sufficient signal-to-noise ratio) are a fast (several MHz) control BWO voltage supply (i.e., BWO frequency) and obtaining a stable

<sup>†</sup> The  $\text{SO}_2$  spectrum was proposed by Drs. J. Bellet and A. Steenbeckeliers.



FIG

operation of the 1  
Fig. 8. To obtain  
for control signa  
5 kHz to 5 MHz  
cathode through  
BWO supply sta  
astatic servosyste  
supply. For faste  
phase-sensitive d  
deviation from &  
Fig. 8). This BWC  
the stabilized 7  
( $\sim 20$  GHz). Nea  
trum cover 3–6 C

At present we e  
the submillimeter  
frequency discrim  
review are made  
high ( $2 \times 10^{-6}$ , i.  
realized. Figure 9  
approximately 1  
ments are used.  
reference oscillat  
spectrum record &  
urements is  $\sim 2$  ;  
manually by the r

ference [13] are two-formed by variation of from 1 up to 5 kV (at a > oscillation frequency frequency dependence a highly stable BWO regulated speed permits gigahertz with a resolution signal (Figs. 4, 5, 18). Determined with an accuracy accorded reference spectrum the well known  $\sim 10^{-6}$  may be achieved by once spectrum and the frequency modulation [2] BWO frequency stab-

synchronous detection observed form of the in the frequency deviation first derivative of the separately recorded lines here is similar to that the form of the square- is the requirements for a. ce signal (obtained by frequency oscillator) the measurements of the he system of frequency ator, the frequency of 100 MHz range. The lier of the last stage of rlier [20, 21]. The last of the lock-in BWO in h the multiplication of ionics of 70 GHz with VO occur. The main frequency (after obtain- a fast (several MHz) and obtaining a stable enbeckeliers.

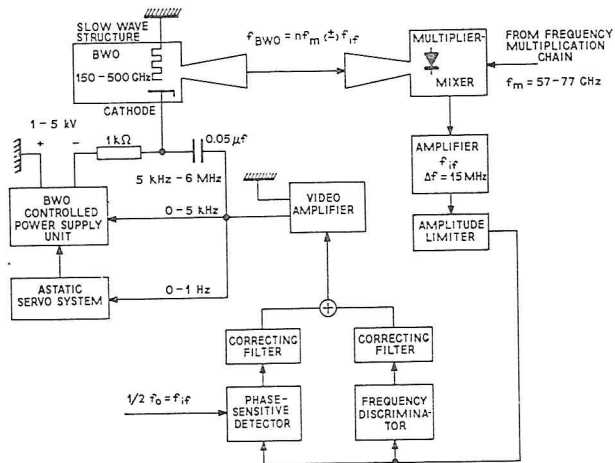


FIG. 8. Phase lock-in circuit of the submillimeter BWO.

operation of the lock-in system. The BWO phase lock-in circuit is given in Fig. 8. To obtain a fast time response of the BWO supply, different channels for control signals with different frequencies are used. Frequencies from 5 kHz to 5 MHz from the video amplifier are applied directly to the BWO cathode through the capacitor. Frequencies of 0 to 5 kHz pass through the BWO supply stabilization circuit. For the lowest (0-1 Hz) frequencies an astatic servosystem is used which drives the potentiometer of the voltage supply. For faster response of the lock-in system the error signal from the phase-sensitive detector is corrected by the first derivative of the phase deviation from a simultaneously operated frequency discriminator (see Fig. 8). This BWO phase lock-in system provides the continuous scanning of the stabilized 70 GHz BWO over the whole range of frequencies ( $\sim 20$  GHz). Near 500 GHz the regions of the continuously scanned spectrum cover 3-6 GHz for one adjustment of the stabilization system.

At present we employ in the RAD a simplified variant of the last stage of the submillimeter BWO frequency stabilization system including only the frequency discriminator [22]. All frequency measurements presented in this review are made with such a simplified system, which permits a sufficiently high ( $2 \times 10^{-6}$ , i.e., defined by Doppler broadening) resolving power to be realized. Figure 9 shows a record of an  $N_2O$  line, the dip on which is approximately 1 MHz in width. Two methods of line frequency measurements are used. In one method, i.e., that with the linear scanning of the reference oscillator frequency by a motor, the frequency is marked on the spectrum record according to counter readings. The accuracy of such measurements is  $\sim 2 \times 10^{-6}$ . In the other method, the BWO frequency is tuned manually by the reference oscillator to the line center and then the frequency

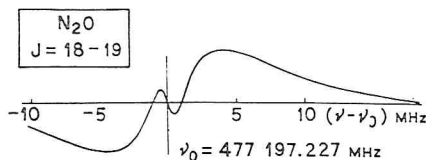


FIG. 9. The record (in the form of the first derivative of the absorption profile) of the rotational transition  $^{14}\text{N}_2\text{O}$  in the ground vibrational state with a dip in the center. Both RAD cells are filled with  $\text{N}_2\text{O}$ . The spectrum is recorded only in the second cell. The dip (1 MHz in width) is due to the absorption of radiation in the first cell, in which the pressure is considerably lower than in the second one.

of the oscillator is counted. For convenience, the lines are observed as first derivatives of absorption profiles, and adjusting the frequency to the line center corresponds to a zero RAD output. The accuracy of this method is better than  $1 \times 10^{-7}$ . The frequencies of  $^{14}\text{N}_2\text{O}$  ground state lines measured by the latter method are given in Table II; the rms deviation of the results amounts to  $2 \times 10^{-8}$  of the relative uncertainty.

#### 2.4. INTENSITY MEASUREMENTS

The value of the RAD output signal may be written as

$$A = KP_0[1 - \exp(-\gamma l)] \quad (16)$$

where  $K$  is an apparatus constant which does not depend on the frequency. Due to the fact that the power of the BWO radiation depends on the frequency, relative intensities of lines observed in the spectrum may differ from their true values. The use of two RAD cells, through which the radiation flux

#### 2.2 NEW METHOD

passes successively, permits the second with a gas BWO frequency per unit reference spectra on. The relation between  $v_2$  of the reference spectrum and theoretical intensity Eq. (16) with  $\gamma l \ll 1$ , is

As a result we may obtain (in relative units) on the intensities of lines of the dependence on the frequency help of the  $\text{SO}_2$  spectrum with the RAD is relatively working with a subrectangular contact diode receiving conditions are mainly the point-contact

To measure the absorption cells are filled with the different. The pressure is considerably smaller than in the second cell. Here the transition line in the first cell and in the center of

TABLE II

The Frequencies of  $^{14}\text{N}_2\text{O}$  Transitions in the Ground Vibrational State

$J \rightarrow J + 1$	$v^{\text{meas}} \pm \Delta v^{\text{meas}}$ (kHz)	$v^{\text{calc}} \pm \Delta v^{\text{calc}}$ kHz	$v^{\text{meas}} - v^{\text{calc}}$ kHz
4 → 5	125 613 696 ± 5.5	125 613 696 ± 2.8	0
5 → 6	150 735 046 ± 6.7	150 735 041 ± 3.2	+ 5
6 → 7	175 855 623 ± 7.8	175 855 626 ± 3.6	- 3 [35]
9 → 10	251 211 557 ± 17	251 211 553 ± 4.2	+ 4
11 → 12	301 442 700 ± 20	301 442 714 ± 4.2	- 14
11 → 12	301 442 713 ± 13	301 442 714 ± 4.2	- 1
12 → 13	326 556 070 ± 13	326 556 076 ± 4.1	- 6
15 → 16	401 885 784 ± 13	401 885 774 ± 4.9	+ 10 this
16 → 17	426 991 784 ± 13	426 991 788 ± 5.7	- 4 work
17 → 18	452 095 648 ± 13	452 095 648 ± 6.9	0
18 → 19	477 197 227 ± 13	477 197 227 ± 8.6	0

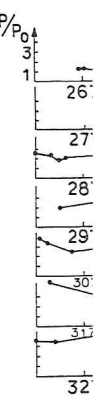


FIG. 10. Experimental record of the reference spectrum

passes successively, permits one to correct the relative line intensities on the record. For this purpose one of the cells is filled with the gas investigated and the second with a gas with known absorption coefficients. Scanning the BWO frequency permits a synchronous record of the investigated and the reference spectra on the chart paper of a two-pen recorder (Fig. 6). The relation between the BWO power at the frequencies of the lines  $\nu_1$  and  $\nu_2$  of the reference spectrum is easy to obtain by comparison of experimental and theoretical intensity relations for the chosen reference lines. From Eq. (16) with  $\gamma l \ll 1$ , it follows that

$$A_1 \gamma_2 / A_2 \gamma_1 = P_0(\nu_1) / P_0(\nu_2). \quad (17)$$

As a result we may obtain a diagram of BWO radiation power dependence (in relative units) on the frequency, which permits us to correct the relative intensities of lines of the spectrum investigated. An example of BWO power dependence on the frequency in the range 267–336 GHz obtained with the help of the  $\text{SO}_2$  spectrum is given in Fig. 10 [23]. The dependence obtained with the RAD is relatively smooth, which is rather unexpected for everyone working with a submillimeter BWO, oversized waveguide, and a point-contact diode receiver. Sharp peaks of the power observed under these conditions are mainly due to interference in the microwave elements, including the point-contact detector, but not to the BWO.

To measure the absolute values of the absorption coefficients both RAD cells are filled with the same sample gas, but the gas pressures in the cells are different. The pressure in the first cell along the radiation path is considerably smaller than in the second one. The signal record is made only in the second cell. Here the line observed has a dip due to the narrow absorption line in the first cell. The signal values from the line outside the dip  $A_1$  and in the center of the dip  $A_2$  are easily associated with the absorption

absorption profile) of the  
in a dip in the center. Both  
in the second cell. The dip  
ell, in which the pressure is

s are observed as first  
frequency to the line  
accuracy of this method is  
ground state lines  
the rms deviation of the  
ity.

n as

(16)

end on the frequency.  
depends on the frequency.  
spectrum may differ from  
which the radiation flux

#### Vibrational State

$\nu^{\text{meas}} - \nu^{\text{calc}}$ kHz
0
+ 5
- 3 > [35]
+ 4
- 14
- 1
- 6
+ 10 this
- 4 work
0
0

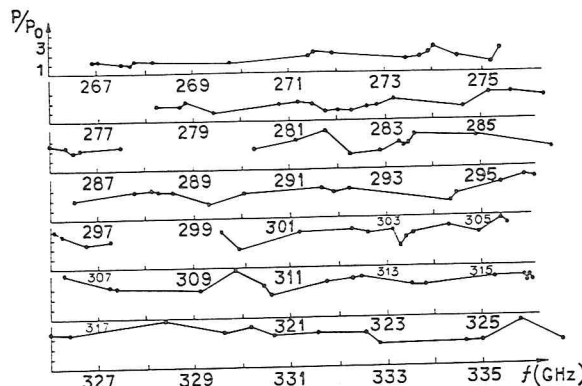


FIG. 10. Experimental dependence of BWO power on the frequency, obtained from the record of the reference  $\text{SO}_2$  spectrum.

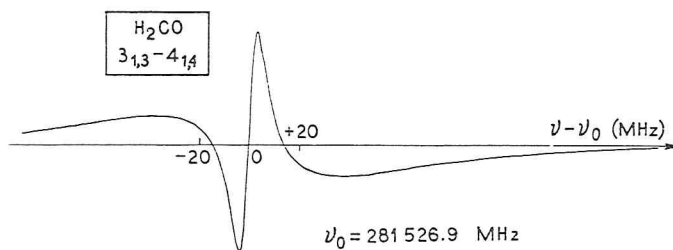


FIG. 11. The record (in the form of the first derivative of the absorption profile) of the rotational transition  $3_{1,3}-4_{1,4}$  of  $\text{H}_2\text{CO}$  in the ground vibrational state ( $\nu \sim 281$  GHz) obtained to measure the absorption coefficient. The dip in the center is due to the absorption in the cell placed before the detector cell (analogous to Fig. 9). The measured absorption coefficient is equal to  $5.9 \times 10^{-2} \text{ cm}^{-1}$ .

coefficient  $\gamma$  and with the length of the first cell  $l_1$ :

$$\gamma = (1/l_1) \ln(A_1/A_2). \quad (18)$$

The possibility of observation in the submillimeter range of lines with a large optical depth ( $\gamma l \geq 1$ ) removes one of the main sources of error in the measurement of the absorption coefficient in the centimeter range—the reflections from the cell ends. Figure 11 gives a record of a line with a dip. The line is recorded with a stabilized BWO as a first derivative of the absorption profile. The absorption line profile is then found by numerical integration. The integrated absorption coefficient of the line is also easily determined from the record with the frequency markers.

## 2.5. THE USE OF LARGE POWER RADIATION SOURCES

Practical experiments on the use of large power radiation sources in the RAD have been carried out in the range of 34 GHz ( $\lambda \sim 8$  mm) at power levels up to  $10^3$  W [24]. As the source of large power coherent radiation, a cyclotron resonance maser (CRM) [25] is used. A calorimeter power meter is placed after the cell (matched load), and the windows and the membrane of the microphone are protected from the large radiation power. The cell has mica windows; a section of waveguide operated beyond cutoff connects the cell with the microphone. The choice of samples investigated is limited due to the limited CRM tuning range. In particular, the transition  $6_{1,5}-6_{1,6}$  of HCOOH is observed at the frequency 34 378.86 MHz. The absorption coefficient of this transition in pure HCOOH vapor  $\gamma_0 = 5.4 \times 10^{-6} \text{ cm}^{-1}$ ; the transition matrix element is nearly 0.1 D. The line width is chosen sufficiently large to prevent saturation up to power levels of the order of  $10^3$  W and is equal to 70 MHz between half-intensity points. Broadening is

FIG. 12. RAD signal ( $6_{1,5}-6_{1,6}$  transition in corresponds to the modu amplification coefficient is determined from this rec

achieved by the addition coefficient of the from measurements in 300 GHz region obs with CRM. The att absorption coefficie  $\gamma = 8.4 \times 10^{-8} \text{ cm}^{-1}$

Figure 12 shows  $6_{1,5}-6_{1,6}$  HCOOH 1 CRM radiation (the RAD receiver noise tion is switched off, the presence or ab signal value increas RAD sensitivity va coefficient from Fig stant of 1 sec. The c of magnitude highe

FIG. 13. The depende (relative units) at the cer 70 MHz linewidth.

$\nu - \nu_0$  (MHz)

absorption profile) of the state ( $\nu \sim 281$  GHz) obtained due to the absorption in the cell. The absorption coefficient is

(18)

ge of lines with a large s of error in the measurement—  
meter range—the d of a line with a dip.  
first derivative of the n found by numerical  
the line is also easily  
ers.

diation sources in the ( $\lambda \sim 8$  mm) at power coherent radiation, a meter power meter is and the membrane of n power. The cell has and cutoff connects the stigated is limited due transition  $6_{1,5}-6_{1,6}$  of 4Hz. The absorption  $\gamma = 5.4 \times 10^{-6} \text{ cm}^{-1}$ ; line width is chosen levels of the order of points. Broadening is

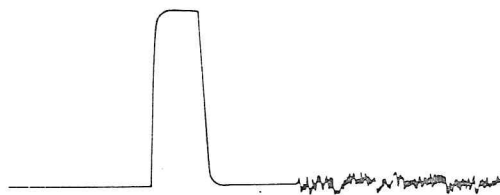


FIG. 12. RAD signal at the center of a line with absorption coefficient  $8.4 \times 10^{-8} \text{ cm}^{-1}$  ( $6_{1,5}-6_{1,6}$  transition in HCOOH diluted by  $N_2O$ ) at 1 kW radiation power. The step corresponds to the modulation switched on and off. On the right there is RAD noise when the amplification coefficient is increased 100 times. The time constant is 1 sec. The RAD sensitivity determined from this record is  $(1-2) \times 10^{-11} \text{ cm}^{-1}$ .

achieved by the addition of foreign gas ( $N_2O$ ). The decrease of the absorption coefficient of the HCOOH line due to dilution by  $N_2O$  is determined from measurements of the signal from known  $N_2O$  and HCOOH lines in the 300 GHz region observed in the same cell before and after the experiment with CRM. The attenuation coefficient is equal to  $1.54 \times 10^{-2}$  and the absorption coefficient of the line observed after dilution is given by  $\gamma = 8.4 \times 10^{-8} \text{ cm}^{-1}$ .

Figure 12 shows on the left the RAD signal value at the center of the  $6_{1,5}-6_{1,6}$  HCOOH line diluted by  $N_2O$  using amplitude modulation of the CRM radiation (the radiation power is 1 kW), and shows on the right the RAD receiver noise when the amplification is increased 100 times (modulation is switched off, radiation is present). The noise level does not depend on the presence or absence of the radiation passing through the cell and the signal value increased proportional to the radiation power (Fig. 13). The RAD sensitivity value defined by the minimum detectable absorption coefficient from Fig. 12 is equal to  $(1-2) \times 10^{-11} \text{ cm}^{-1}$  with a time constant of 1 sec. The calculated sensitivity value at  $P_0 = 10^3 \text{ W}$  is three orders of magnitude higher and to our regret has not been achieved due to poor

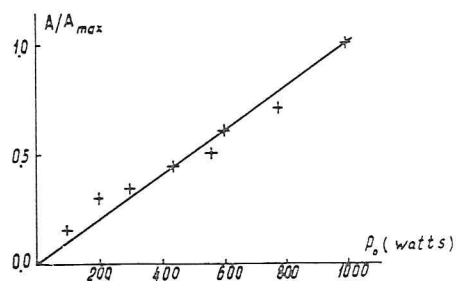


FIG. 13. The dependence on the power of the radiation source (in watts) of the RAD output (relative units) at the center of the  $6_{1,5}-6_{1,6}$  HCOOH line with the matrix element 0.1 D and 70 MHz linewidth.

construction of the microphone, the cell, and the electronic circuit in these early experiments. However, the sensitivity obtained exceeds by more than an order of magnitude the sensitivity of common microwave spectrometers in this region [2, 16]. The use of improved cells and detectors must give further increase of the RAD sensitivity.

Besides the resonance signal from the spectral line (the line profile is observed "point-by-point" during manual tuning of the CRM frequency) a small signal of nonresonant character is observed, the nature of which is not clear presently. To observe only the resonance part of the signal it is sufficient to use frequency modulation of the radiation instead of the amplitude modulation used in the experiments.

This "brute force" method of sensitivity increase is probably the only one available for obtaining such a high sensitivity in spectrometers in the submillimeter and far-infrared regions of the spectrum since RAD sensitivity does not depend on the frequency and there are powerful (though almost nontunable) sources of radiation [26].

Thus, it is experimentally confirmed that the sensitivity of the RAD spectrometer does exceed the sensitivity of the common microwave spectrometers. In practice, such a method of sensitivity increase is not applicable to all spectra; it is better applied in the case of isolated spectral lines with small matrix elements of the transition dipole moment. A good object may be "forbidden" spectra [27-29]. The possibility of action on the molecules by the strong radiation field (including the resonant frequency of the line observed) opens a new field of investigation in microwave spectroscopy (for example, the observation of purely rotational spectra of nonpolar molecules, for which the dipole moment is induced by the field, two-quantum processes, etc.). These problems are considered in detail in Section 4.

### 3. Description of Spectra by the Correlation Matrix Technique

In microwave spectroscopy the experimentally observed spectra are described by theoretical models containing phenomenological parameters. The search for these parameters ("the inverse problem" of spectroscopy) is carried out on the basis of certain fit criteria for the experimental and the calculated spectra. The model parameters obtained are functions of experimental data with random errors, i.e., they also have random errors. Usually the model parameters are statistically dependent. However, in the literature their statistical properties (under the normal distribution law) are characterized by dispersions only, i.e., by the diagonal elements of the parameter correlation matrix. This information is not complete and, in particular, may lead to incorrect accuracy estimates for spectral line frequencies calculated from the model parameters determined (in the "direct problem"), especially

when using experimental development and correlation techniques in the process.

### 3.1. REDUCTION C

The problem of parameters is one of the most difficult problems in molecular spectroscopy. The number of parameters in the molecule given by the spectrum depends on the concrete set of experiments. In the range, the accuracy of the spectrum depends on the range of the spectrum. For that reason it is necessary to process the data. Moreover, it will be necessary to determine from the spectrum the values of the parameters. The elimination of the problem of search for the parameters is taking complete account of the inverse problem.

Let  $X_1, X_2, \dots$  be random variables with independent distributions with mean  $\xi_1, \xi_2, \dots, \xi_N$  respectively. Let  $\eta$  depend on the  $X_i$ 's. We want to find the maximum of the function  $\eta$ , which is equivalent to finding the maximum of the function

where  $\sigma_i^2$  is the di-

Let us assume that a rough solution to the exact solution one functional [Eq. (19)]

<sup>†</sup> This problem is typified by the following:

tronic circuit in these exceeds by more than rowave spectrometers d detectors must give

ne (the line profile is he CRM frequency) a nature of which is not rt of the signal it is i instead of the ampli-

probably the only one ometers in the submil- RAD sensitivity does hough almost nontun-

vity of the RAD spec- ion microwave spec- rease is not applicable ted spectral lines with nt. A good object may tion on the molecules frequency of the line ave spectroscopy (for of nonpolar molecules, o-quantum processes, ion 4.

### matrix Technique

observed spectra are nological parameters. "n" of spectroscopy) is experimental and the re functions of exper- andom errors. Usually ever, in the literature uation law) are charac- ients of the parameter and, in particular, may frequencies calculated problem"), especially

when using experimental data from the lower frequency range.<sup>†</sup> The development and the practical application of algorithms using the matrix correlation technique shows that this technique permits some new possibilities in the processing of experimental data. Two of them are given below.

#### 3.1. REDUCTION OF THE NUMBER OF PARAMETERS

The problem of the molecular spectrum description by a minimal number of parameters is of significant interest. As an example of an analytical solution of this problem one may point to the latest reduction of the number of parameters in the pure rotational Hamiltonian model for an asymmetric top molecule given by Watson [30]. However, the minimal number of model parameters necessary and sufficient for a description of the experimental spectrum depends both on the model chosen for the molecule and on the concrete set of experimental data (the branches of the transitions observed, the range, the accuracy, and the resolving power of the spectrometers, etc.). For that reason it is impossible using analytical methods to indicate before processing the data which parameters may be neglected in the spectral fit. Moreover, it will be shown below that a large uncertainty in a parameter as determined from the experimental data may not be a sufficient criterion for elimination of this parameter. Below we give the general solution of the problem of searching for the model parameters needed for the spectral fit, taking complete account of the statistical properties of the solution to the inverse problem.

Let  $X_1, X_2, \dots, X_N$  be a set of experimental data for the assigned transitions with independent random errors distributed over the normal law, and let  $\xi_1, \xi_2, \dots, \xi_N$  be theoretical analogs of the experimental data which depend on the phenomenological parameters  $A_1, A_2, \dots, A_s$ . The criterion for maximum confidence leads to a requirement on the model parameters which is equivalent to the prescription of the method of least squares [31]

$$\phi(A) = \sigma^2 \sum_i \{[X_i - \xi_i(A)]/\sigma_i\}^2 = \min, \quad (19)$$

where  $\sigma_i^2$  is the dispersion of the random value  $X_i$ ,  $\sigma^2 = 1/\sum_i (1/\sigma_i)^2$  is the normalization constant.

Let us assume that we know (for example, from structural considerations) a rough solution to the inverse problem  $A^0$ , such that in the search for the exact solution one may linearize the theoretical dependences  $\xi_i(A)$ . Then the functional [Eq. (19)] may be transformed to the form

$$\phi(a) = \langle a | V | a \rangle - 2\langle t | a \rangle + d^2. \quad (20)$$

<sup>†</sup> This problem is typical presently for the submillimeter range, since experimental investigations are not numerous.

Here  $|a\rangle = |A - A^0\rangle$  is the vector of the model parameter differences from their initial estimates,

$$\begin{aligned} V &= \sigma^2 \sum_i |\alpha^{(i)}\rangle \langle \alpha^{(i)}| / \sigma_i^2 \\ |t\rangle &= \sigma^2 \sum_i \{[X_i - \xi_i(A^0)]/\sigma_i^2\} |\alpha^{(i)}\rangle \\ d^2 &= \sigma^2 \sum_i \{[X_i - \xi_i(A^0)]/\sigma_i\}^2, \end{aligned} \quad (21)$$

where  $|\alpha^{(i)}\rangle$  is the gradient of  $\xi_i(A)$  in the space of parameters  $a_k$ .

The operator  $V$  is a symmetric operator in the space of finite dimensions. For this class of operators there are good iterational algorithms (see, for example, reference [32]) for searching for the orthonormal system of eigenvectors  $\{g_n\}$  and the eigenvalues  $\{\lambda_n\}$  corresponding to them.<sup>†</sup> The solution to Eq. (20) is found in the form

$$|a\rangle = C_n |g_n\rangle. \quad (22)$$

We may show [33] for the coefficients  $C_n$  minimizing the functional [Eq. (20)] that: (i)  $C_n = \langle t | g_n \rangle / \lambda_n$ , ( $\lambda_n \neq 0$ ); (ii) the coefficients  $C_n$  are normally distributed statistically independent values with dispersions  $\sigma^2 / \lambda_n$ . The value  $C_n$  corresponding to  $\lambda_n \neq 0$  fixes a certain linear combination of parameters. Indeed, from Eq. (22) it follows

$$C_n = \langle g_n | a \rangle = g_n^{(n)} a_n. \quad (23)$$

Such linear combinations of the parameters we shall call "determinable." Further, it is convenient to assume that the vector of initial estimates of the model parameters  $A^0$  is included in the set of experimental data  $\{X_i\}$ . It is necessary to distinguish (in considering the above statistical properties of the coefficients  $C_n$ ) the point chosen for expanding in the space of the model parameters and the random point  $A^0$ . As a result, a functional is obtained for which all eigenvalues  $\lambda_n$  are strictly positive, i.e., all linear combinations of the form [Eq. (23)] are determinable. Then, an unambiguous set of the model parameters is given in the form of Eq. (23). Since, in the general case, the directions of eigenvectors do not coincide with the direction of the coordinate axes in the model parameter space, there is a correlation between

<sup>†</sup> In order to decrease the value  $\lambda_{\max}/\lambda_{\min}$  in practical use of the method, it is useful to normalize the parameters  $a_k$  in such a way that the diagonal elements of the operator  $V$  will be of the same order of magnitude.

FIG. 14. Correlation situation. The case is shown when the  $\lambda_1$  and  $\lambda_2$  are quite different (correlation of the parameters  $(\eta_1, \eta_2 < 1)$ ). Upon eliminating the random values  $a_k$

$B =$

which is convenient to choose the matrix. It is necessary to eliminate the parameter  $A_2$  or  $A_1$

$\eta_k$

is insufficient in those cases and other parameter cases of a two-dimensional problem. Parameters are small enough both parameters of errors of the coefficients and the measured spectrum (for example,  $A_1 = 0$ ), which almost does not change

<sup>†</sup> In the solution of the inverse problem, calculated line frequencies of the parameters. It may be shown that the nondiagonal terms

differences from

(21)

parameters  $a_k$ .  
finite dimensions.  
algorithms (see, for  
ul system of eigen-  
† The solution to

(22)

ng the functional  
oefficients  $C_n$  are  
dispersions  $\sigma^2/\lambda_n$ .  
ar combination of

(23)

ll "determinable."  
al estimates of the  
ital data  $\{X_i\}$ . It is  
al properties of the  
pace of the model  
onal is obtained for  
ar combinations of  
biguous set of the  
in the general case,  
ne direction of the  
correlation between

method, it is useful to  
of the operator  $V$  will be

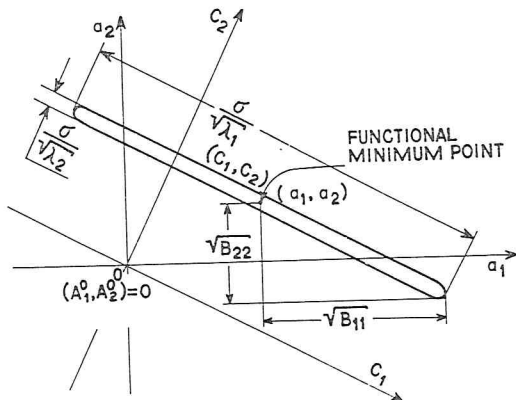


FIG. 14. Correlation surface in two-dimensional space of the model parameters  $A_1$  and  $A_2$ . The case is shown when the accuracy of definition of the statistically independent coefficients  $C_1$  and  $C_2$  is quite different  $\{[(\Delta C_2)^2]^{1/2} = \sigma/\lambda_2^{1/2} \ll [(\Delta C_1)^2]^{1/2} = \sigma/\lambda_1^{1/2}\}$ . This leads to a strong correlation of the parameters  $A_1$  and  $A_2$  and (in this example) to their bad definition ( $\eta_1, \eta_2 < 1$ ). Upon eliminating either of the two parameters ( $A_1 = 0$  or  $A_2 = 0$ ) the experimental and theoretical spectral fit practically does not change, but the remaining parameter ( $A_2$  or  $A_1$ ) is well determined ( $\eta_2 \gg 1$  or  $\eta_1 \gg 1$ ).

the random values  $a_k$ †

$$B = |\overline{a - \bar{a}}\rangle\langle a - \bar{a}| = \sum_n (\sigma^2/\lambda_n) |g_n\rangle\langle g_n|, \quad (24)$$

which is convenient to characterize with the help of the correlation coefficient matrix. It is necessary to note that in determining the significance of the parameter  $A_k$  the commonly used quantity

$$\eta_k = [A_k^0 + a_k]/[(\Delta a_k)^2]^{1/2} = A_k/(B_{kk})^{1/2} \quad (25)$$

is insufficient in those cases when there is a strong correlation between  $A_k$  and other parameters. Figure 14 illustrates this situation for the simplest case of a two-dimensional ( $S = 2$ ) model space. The initial values  $\eta$  for both parameters are smaller than unity ( $A^0 = 0$  for simplicity). However, excluding both parameters ( $A_1 = A_2 = 0$ ) leads to a solution far beyond the limits of errors of the coefficients  $C$ , i.e., to poor agreement between the calculated and the measured spectra. But one may exclude one of the parameters (for example,  $A_1 = 0$ ), which leads to a good definition of the parameter  $A_2$  and almost does not change the spectrum fit.

† In the solution of the direct problem it is significant to estimate the dispersions of the calculated line frequencies arising from uncertainties in the determination of the model parameters. It may be shown that  $(\xi - \bar{\xi}_i)^2 = \langle a^i | B | a^i \rangle$  depends significantly (in the general case) on the nondiagonal terms of the correlation matrix [33].

In order to formulate exactly the criterion for excluding the parameter  $A_k$  at  $\eta_k \sim 1$ , it is necessary to consider how much the functional obtained differs from its minimal value. One may show that the fit of the experimental and the theoretical spectra becomes  $m$  times worse ( $\phi^{1/2} = m\phi_{\min}^{1/2}$ ) upon change of one of the coefficients  $C_n$  from the value at which the functional minimum is realized to a value  $C_n + \delta C_n$ , where  $\delta C_n$  is equal to

$$|\delta C_n|/[(\Delta C_n)^2]^{1/2} \simeq [(m^2 - 1)(N - S)]^{1/2}. \quad (26)$$

In fact, the maximal possible change of the parameter  $A_k$  here satisfies  $|\delta A_k|/[(\Delta A_k)^2]^{1/2} \sim |\delta C_n|/[(\Delta C_n)^2]^{1/2}$ , where the number  $n$  is chosen to correspond to the coefficient  $C_n$  which makes the main contribution to the uncertainty of the parameter  $A_k$ . For  $m = 1.5$ ,  $N = 100$ ,  $S = 9$ , we obtain  $|\delta C_n|/[(\Delta C_n)^2]^{1/2} \sim 11$ , i.e., the fit becomes one and a half times worse when the parameter change exceeds by more than ten times the rms error. Equations (25) and (26) give the criterion for excluding the parameter  $A_k$  at the given value  $m$  for  $\eta_k \gtrsim 1$ .

It should be noted that in the presence of correlation between the parameters  $\{A\}$ , the solution of the problem of parameter round-off is complicated as well. The difficulty is that the round-off leads in the general case to uncorrelated changes of the parameters. The upper limit for the worsening of the fit may be estimated from the expression [Eq. (26)] if we assume that the round-off gives rise to a shift of the solution in the space of the model parameters along the direction  $C_n$  with the minimal value  $[(\Delta C_n)^2]^{1/2}$ .

### 3.2. "SNOWBALL" LINE ASSIGNMENT

The use of continuous broadband records of molecular absorption spectra for a number of purposes begins with the most difficult stage of the line assignment, i.e., with the definition of the quantum numbers of the initial and the final energy levels for those observed transitions described by the molecular model chosen. The large number of experimental data contained in the spectral records gives rise to the problem of developing a sufficiently general and convenient method for automating the assignment. At present the methods using Loomis-Wood diagrams [34]<sup>†</sup> are most advanced in this direction. However, their efficiency decreases when passing from spectra of linear and symmetric top molecules to spectra of the most common asymmetric top molecules. An outline of an assignment method suitable for the rotational spectrum of any of the above types of molecules is given below. The basis of this method is an easily automated regular algorithm, using

<sup>†</sup> The application of graphical plots in the interpretation of the rotational structure of the vibration rotation bands in the infrared was first proposed and extensively used at The Ohio State University. (See Scott and Narahari Rao, [34a], Gherzetti and Narahari Rao [34b], and Mantz and Narahari Rao [34c], and Narahari Rao [34d].

## 2.2 NEW METHODS I

rough initial estimates for continuous record of the frequency range to permit assigned transition. In cc transition assignment, the

The frequency of one determine all the model parameters their linear combinations definition of one direction definition of the set of parameters error of measurement of the orthogonal to the defined by the accuracy of the inverse solution of the inverse problem parameters  $A_1, A_2, \dots, A_n$  necessary to take account

The substitution of the problem permits us first, to find the transition with an uncertain second, to predict (with frequencies for those transitions of model parameters the same class. Some of them Note that transitions of intensity and this makes classification of transitions calculation is, in fact, the "ordering parameters".

Let us consider, for example, assignment of the continuous frequency range of 260 cm<sup>-1</sup> for a model of the nonrigid molecule. The rotational and 6 centrifugal problem solution are: rotational relative error of the order of the frequency of the ground state of <sup>32</sup>S<sup>16</sup>O

<sup>†</sup> The computer program takes account the statistical properties of the orthogonal to the direction of the uncertainties of the initial estimate than for the defined direction magnitude larger).

ing the parameter  $A_k$  functional obtained of the experimental  $\phi^{1/2} = m\phi_{\min}^{1/2}$ ) upon which the functional equal to

$$|^{1/2}. \quad (26)$$

ter  $A_k$  here satisfies number  $n$  is chosen to contribution to the  $S = 9$ , we obtain half times worse when the rms error. Equa- parameter  $A_k$  at the

ion between the par- ter round-off is com- d in the general case limit for the worsen- Eq. (26)] if we assume on in the space of the imal value  $[(\Delta C_n)^2]^{1/2}$ .

ilar absorption spectra difficult stage of the line numbers of the initial tions described by the imental data contained developing a sufficiently assignment. At present e most advanced in this passing from spectra of ie most common asym- method suitable for the molecules is given below. regular algorithm, using

the rotational structure of the extensively used at The Ohio and Narahari Rao [34b], and

rough initial estimates for the model parameters and their uncertainties, a continuous record of the rotational spectrum in a sufficiently broad frequency range to permit observing its general structure, and one initial assigned transition. In conjunction with a method for finding the initial transition assignment, the given algorithm solves this problem completely.

The frequency of one assigned transition is clearly insufficient to determine all the model parameters; nevertheless, it does fix the value of one of their linear combinations of the form [Eq. (23)]. This corresponds to the definition of one direction in the space of parameters along which the variation of the set of parameters is limited by a small interval defined by the error of measurement of the assigned transition frequency. In the subspace orthogonal to the defined direction the parameter variations are limited only by the accuracy of the initial estimates, i.e., they are rather large. A full solution of the inverse problem is written then in the form of a set of parameters  $A_1, A_2, \dots, A_s$  and their correlation matrix; here it is absolutely necessary to take account of the correlation effects.

The substitution of the full solution obtained as initial data into the direct problem permits us first, to reproduce the frequency of the initially assigned transition with an uncertainty equal to the uncertainty of measurement; second, to predict (with an accuracy lower, but sufficient for assignment) frequencies for those transitions determined by almost the same combination of model parameters. We shall refer to such transitions as transitions of the same class. Some of them may be assigned in addition to the initial one. Note that transitions of the same class usually have the same order of intensity and this makes easier their assignment in a dense spectrum. The classification of transitions according to the accuracy of their frequency calculation is, in fact, the automatic choice of the variation rule of the "ordering parameters" considered in reference [34].

Let us consider, for example, the results of applying the algorithm to the assignment of the continuous record of the  $\text{SO}_2$  rotational spectrum in the frequency range of 260–370 GHz obtained with the RAD. A theoretical model of the nonrigid asymmetric top is used containing 9 parameters (3 rotational and 6 centrifugal constants). The initial data for the inverse problem solution are: rotational constants differing from their true values by a relative error of the order of  $10^{-2}$ , centrifugal constants equal to zero, and the frequency of the assigned transition  $10_{1,9}-11_{2,10}$  in the spectrum of the ground state of  ${}^3\text{S}{}^1 {}^{16}\text{O}_2$  equal to  $323\ 046.4 \pm 0.2$  MHz.<sup>†</sup>

<sup>†</sup> The computer program used for the solution of the inverse problem does not take into account the statistical properties of the initial parameter estimations. Variations in the subspace orthogonal to the direction defined by one experimental frequency are not limited by the uncertainties of the initial estimates of the parameters, but they are simply chosen much larger than for the defined directions (in the concrete example considered, they are 4 orders of magnitude larger).

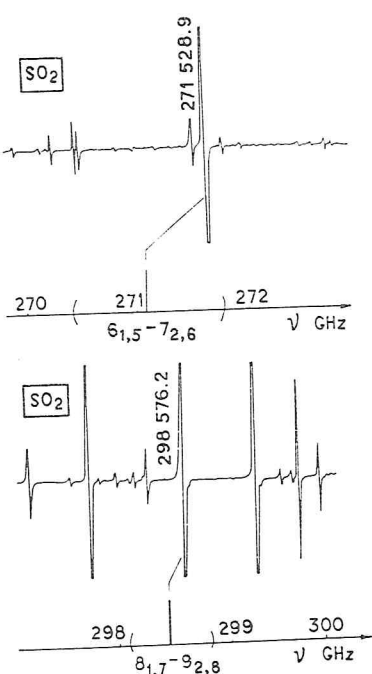


FIG. 15. The search for SO<sub>2</sub> lines on the experimental spectrum record from predictions in the first cycle of the assignment. Brackets indicate the accuracy of the predicted frequencies. The assignments obtained are shown in the figure.

The spectrum calculation in the direct problem permits the location of the additional transitions 4<sub>1,3</sub>-5<sub>2,4</sub>, 6<sub>1,5</sub>-7<sub>2,6</sub>, 8<sub>1,7</sub>-9<sub>2,8</sub>, 12<sub>1,11</sub>-13<sub>2,12</sub>, 14<sub>1,13</sub>-15<sub>2,14</sub>, belonging to the same class as the initial one, since their frequencies are defined with better accuracy than for all other transitions. Figure 15 gives parts of the recorded spectrum close to the calculated transition frequencies. One may without doubt assign the experimental transitions 298 576.2 ± 0.2 MHz and 271 528.9 ± 0.2 MHz to the calculated ones 298 464 ± 400 MHz and 6<sub>1,5</sub>-7<sub>2,6</sub> ( $v_{\text{calc}} = 271 079 \pm 8_{1,7}-9_{2,8}$  ( $v_{\text{calc}} = 298 464 \pm 400$  MHz)) and 6<sub>1,5</sub>-7<sub>2,6</sub> ( $v_{\text{calc}} = 271 079 \pm 620$  MHz), taking into account their similar intensity. From the results of calculations for transitions of the given class one may plot a diagram of differences between the theoretical frequencies and the experimental frequencies closest to them, analogous to reference [34], and mark the error limits of the theoretical frequencies. This gives a natural criterion for the correct assignment (see Fig. 16).

A decrease in accuracy of transition frequency prediction in a given class occurs because the frequencies are defined by more and more different parameter combinations, i.e., directions fixed in the space of parameters by transitions of the same class are close to each other, but they do not coincide.

#### TRANSITION IDENTIFICATION

4 <sub>1,3</sub> -5 <sub>2,4</sub>
6 <sub>1,5</sub> -7 <sub>2,6</sub>
8 <sub>1,7</sub> -9 <sub>2,8</sub>
10 <sub>1,9</sub> -11 <sub>2,10</sub>
12 <sub>1,11</sub> -13 <sub>2,12</sub>
14 <sub>1,13</sub> -15 <sub>2,14</sub>

FIG. 16. The diagram of the first cycle of the assignment of frequency of one assigned transition to frequency predictions. Figures marked by rectangles. N

That is why after assigning frequencies, an increase in accuracy of the next stage occurs. "problem" → "direct problem" frequency values to moment process occurs. Assignments can be assigned to

Let us consider briefly the assignment. A number of experiments which make the estimates for the model frequency range investigation is the most convenient (sensitivity) and identify it with the case, if this initial assignment is predicted on the basis of spectrum, it is convenient to change its experimental frequency is equivalent scheme for the initial assignment by the computer even analogs for the initial small value.

† The word "snowball"

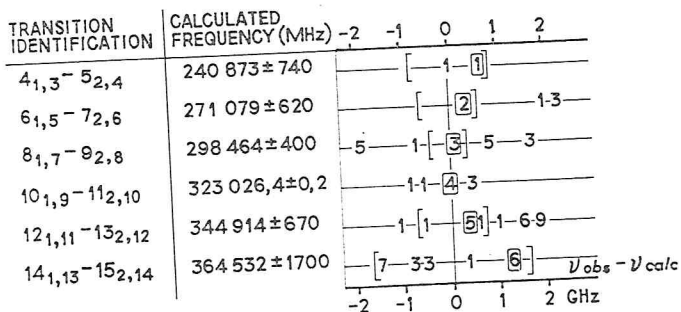


FIG. 16. The diagram of differences of the calculated and the experimental frequencies after the first cycle of the assignment process. The initial information for the first stage is the frequency of one assigned transition  $10_{1,9} - 11_{2,10}$ . Brackets indicate the accuracy of the line frequency predictions. Figures indicate the relative transition intensities. Assigned transitions are marked by rectangles. Note that they form a smooth curve.

That is why after assignment of the new transitions with their experimental frequencies, an increase in information at the input of the inverse problem at the next stage occurs. Upon repetition of the cycle "inverse problem" → "direct problem" → "assignment of additional experimental frequency values to molecular transitions" → "...", a "snowball"† assignment process occurs. After each cycle a larger number of additional transitions can be assigned than was possible in the previous cycle.

Let us consider briefly the method for making the initial transition assignment. A number of experimental methods are known in microwave spectroscopy which make the assignment of a transition easier [2, 4]. Using rough estimates for the model parameters one may predict transitions falling in the frequency range investigated. Let us choose one theoretical transition which is the most convenient for assignment (for example, with the largest intensity) and identify it with one of the possible experimental analogs. In this case, if this initial assignment is not correct and the additional transitions predicted on the basis of this information are absent in the experimental spectrum, it is convenient to consider the same theoretical transition, but to change its experimental analog. Really, the variation of the transition frequency is equivalent to the search over the one parameter. Such a search scheme for the initial transition assignment is efficient enough for realization by the computer even in the case when the number of possible experimental analogs for the initially chosen theoretical transition can not be reduced to a small value.

im record from predictions in the predicted frequencies. The

permits the location of the  $1_{1,7} - 9_{2,8}$ ,  $12_{1,11} - 13_{2,12}$ , initial one, since their for all other transitions. e to the calculated transitions experimental transitions to the calculated ones  $1_{1,7} - 9_{2,8}$  ( $\nu_{calc} = 271\ 079 \pm$  intensity. From the results of e may plot a diagram of s and the experimental e [34], and mark the error natural criterion for the

prediction in a given class re and more different par e space of parameters by r, but they do not coincide.

† The word "snowball" was suggested by Dr. J. T. Hougen.

#### 4. Prospects for Further Investigations with RAD

The development of new experimental methods always stimulates a broadening of the range of investigation. Here future prospects for submillimeter spectroscopy by RAD are briefly described. The results of investigations are only illustrative.

##### 4.1. LOW INTENSITY SPECTRA

RAD provides high sensitivity in the frequency region where rotational lines of a broad class of molecules reach a maximum of intensity [4]. The intensity increase in comparison with the "classic" centimeter range may be several orders of magnitude. As a result, possibilities for observation of low-intensity rotational spectra are highly improved. Low intensity of transitions in a spectrum may be due to a small abundance of molecules in the levels investigated and/or to a small value of the matrix element of the dipole moment inducing the transition. As an example, one may point out transitions between the higher energy levels of molecules and transitions in rare isotopic species in natural abundance; transitions induced by the magnetic dipole moment; "forbidden" transitions [27, 28], etc. For example, with the help of RAD a rotational spectrum of  $^{14}\text{N}_2^{16}\text{O}$  in the frequency range 300–480 GHz has been investigated in the ground and in the higher vibrational states. Figure 3 illustrates observation conditions for rotational transitions of  $^{14}\text{N}^{14}\text{N}^{16}\text{O}$  in the vibrational states (010) at  $589 \text{ cm}^{-1}$ , (020) at  $1178 \text{ cm}^{-1}$ , (030) at  $1767 \text{ cm}^{-1}$ , and for  $^{14}\text{N}^{15}\text{N}^{16}\text{O}$  in the vibrational state (010) in natural abundance. Experimental values of the transition frequencies given in reference [35] together with those obtained by RAD have been used to determine molecular parameters for  $^{14}\text{N}_2^{16}\text{O}$ . The rotational and centrifugal constants and also the correlation coefficients between them for some vibrational states are given in Table III. All quoted errors correspond to a 75% confidence limit. The analogous values from reference [35] are given there for comparison. Accuracy improvements are achieved mainly for the centrifugal constants, which are associated with the increased effects of molecular nonrigidity at the higher frequencies. All the parameters are within the error limits quoted in reference [35]. Figure 17 shows the conditions for observation of lines of the isotopic water molecule species  $\text{H}_2^{18}\text{O}$  and  $\text{H}_2^{17}\text{O}$  in their natural abundances with the help of RAD near 0.538 mm (the lines  $1_{0,1}-1_{1,0}$ ), the line of the main isotopic species  $\text{H}_2^{16}\text{O}$  is limited by the recorder. These transitions are approximately  $10^5$  times more intense than transitions of a water molecule in the centimeter range. The observation of "forbidden" spectra by RAD is advantageous since the intensity of the majority of such spectra sharply increases with frequency (for example, for molecules with a dipole moment due to centrifugal distortion

FIG. 17. The record of  $\text{H}_2^{17}\text{O}$ —0.037%.

[28]) and is also advantageous (for nonpolar symm absent [36]).

A very interesting an free radicals. The stimul small dimensions of the

Rotational and Centrifugal  
G<sub>1</sub>

Vibration state	$B_v \pm \Delta$
00 <sup>0</sup> 0	12 561 63
01 <sup>1</sup> 0	12 561 63
01 <sup>1</sup> d0	12 566 63
01 <sup>1</sup> d0	12 566 63
02 <sup>0</sup> 0	12 590 38
02 <sup>0</sup> 0	12 590 38
02 <sup>2</sup> d0	12 595 0
02 <sup>2</sup> d0	12 595 0
02 <sup>2</sup> c0	12 595 0
02 <sup>2</sup> c0	12 595 0

<sup>a</sup> The constants in the to the formula we use v =

always stimulates a prospects for submili-  
te results of investiga-

gion where rotational n of intensity [4]. The ntimeter range may be ies for observation of Low intensity of transnence of molecules in the ix element of the dipole > may point out transn- and transitions in rare duced by the magnetic . For example, with the in the frequency range and in the higher vibratons for rotational transn-) at 589 cm<sup>-1</sup>, (020) at ) in the vibrational state the transition frequen- ined by RAD have been -O. The rotational and cients between them for uoted errors correspond from reference [35] are s are achieved mainly for i the increased effects of All the parameters are gure 17 shows the cond- molecule species H<sub>2</sub><sup>18</sup>O the help of RAD near isotopic species H<sub>2</sub><sup>16</sup>O is oximately 10<sup>5</sup> times more e centimeter range. The antageous since the inten- eases with frequency (for > to centrifugal distortion

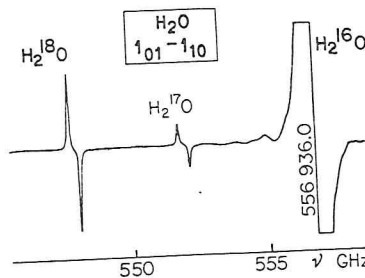


FIG. 17. The record of the rotational transitions of water molecules in the ground vibrational state for different isotopic combinations in natural abundance (H<sub>2</sub><sup>18</sup>O—0.20%· H<sub>2</sub><sup>17</sup>O—0.037%).

[28]) and is also advantageous when the use of Stark modulation is impossible (for nonpolar symmetric top molecules Stark effect of the first order is absent [36]).

A very interesting and large field of study may be the investigation of free radicals. The stimulating advantages here are the high sensitivity and small dimensions of the cell of the RAD.

TABLE III  
Rotational and Centrifugal Constants <sup>14</sup>N<sub>2</sub><sup>16</sup>O and Their Correlation Coefficients in the Ground and Excited Vibrational States

Vibration state	B <sub>v</sub> ± ΔB <sub>v</sub> kHz	D <sub>v</sub> ± ΔD <sub>v</sub> Hz	Correlation coefficient	References
00 <sup>0</sup>	12 561 633.8 ± 0.6	5 282 ± 4	+0.88	[35]
	12 561 633.6 ± 0.3	5 279.5 ± 0.6	+0.86	This work
01 <sup>1c</sup> 0	12 566 636.9 ± 2.0	5 352 ± 12	—	[35] <sup>a</sup>
	12 566 636.2 ± 1.2	5 345.5 ± 2.7	+0.80	This work
01 <sup>1d</sup> 0	12 590 380.2 ± 2.2	5 373 ± 13	—	[35]
	12 590 380.8 ± 0.9	5 377.9 ± 3.1	+0.70	This work
02 <sup>0</sup> 0	12 588 875 ± 19	7 356 ± 110	—	[35]
	12 588 883.1 ± 3.3	7 394.4 ± 5.6	+0.98	This work
02 <sup>2d</sup> 0	12 595 067 ± 15	5 413 ± 97	—	[35]
	12 595 070.2 ± 7.7	5 451 ± 14	+0.95	This work
02 <sup>2c</sup> 0	12 595 061.7 ± 9.1	3 639 ± 57	—	[35]
	12 595 067.6 ± 5.9	3 674 ± 10	+0.95	This work

<sup>a</sup> The constants in the excited vibrational states are recalculated from  $v = 2B_v(J+1) - 4D_v(J+1)\{(J+1)^2 - l^2\}$ <sup>[35]</sup> to the formula we use  $v = 2B_v(J+1) - 4D_v(J+1)^3$ .

## 4.2. BROADBAND SPECTRAL STUDIES

The range of RAD operating frequencies covering nearly 1 THz is comparable to the range of the most intense part of molecular rotational spectra [4]. Earlier, such continuous broadband spectral records were obtained only by the methods of infrared spectroscopy, i.e., with considerably lower sensitivity, resolving power, and accuracy of spectral line frequency measurements. The possibility of observation of broadband continuous spectra by microwave methods has significant advantages for the analysis of spectra. In this case, methods of line assignments using the diagram technique [34] (typical of infrared spectroscopy) may be used effectively, as well as the method described in Section 3.2, etc.

These methods can be applied to the interesting problem of searching for new details in the spectrum not predicted by the initial model of the molecule. As a practical example, we consider the explanation of the residual HCOOH spectrum in the 200–480 GHz range obtained after the elimination of the known lines of the ground state. This problem arose after discovering regular groups of lines in the broad HCOOH spectrum records which are not explained by the initial model of the molecule as an asymmetric top (without the additional interactions). A display of these groups of lines is given in Fig. 18. They are observed before each  $R_x$ -group of the ground state of HCOOH. The line intensities in these groups are 20–30 times smaller than the line intensities in  $R_x$ -groups of the ground state, which would correspond approximately to the intensity of vibrational satellites from the states  $v_7 = 1$  or  $v_9 = 1$ . However, the form of these groups of lines strongly differs from the form of the ground state groups, which makes their identification difficult. The increase in intensity of these groups relative to the intensity of ground state groups upon cell heating confirms the fact that these groups belong to excited states of the HCOOH molecule. The record of the HCOOD spectrum shows groups of lines at the corresponding places in the HCOOD spectrum, which are, however, more similar to the  $R_x$ -groups of the ground state; their intensities also correspond to  $v_7 = 1$  or  $v_9 = 1$ . The atom H (or D) takes part in the  $v_9$  vibration (the out-of-plane motion of the molecule [37]). The difference between HCOOH and HCOOD lies in the fact that the levels  $v_9 = 1$  and  $v_7 = 1$  in HCOOH are much closer than in HCOOD (13 and 54 cm<sup>-1</sup>, respectively [37]).

It is natural to assume that the groups investigated belong to the rotational spectrum of HCOOH in the vibrational states  $v_7 = 1$  and  $v_9 = 1$  perturbed by Coriolis interaction† so strongly that as a result the order of the lines appearing in the  $R_x$ -groups changes. To go further, one must define quantum numbers for each line.

† The presence of Coriolis interaction between the states  $v_7 = 1$  and  $v_9 = 1$  was pointed out in reference [38].

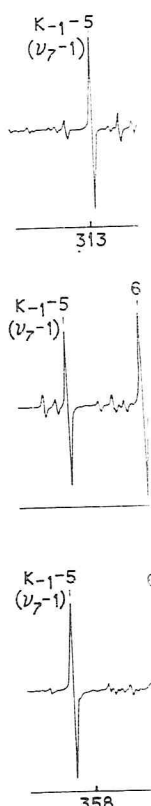


FIG. 18. Groups of lines  
On the right the quantum number  $n$   
belong to the ground vibrational state  
 $v_7 = 1$ , the quantum number  $m$

The close relation of the groups of lines to the  $R_x$ -groups of the ground state establishes the value of the quantum number  $n$ . On account that the dependence of the intensities of the groups of lines upon the temperature of the cell must remain similar for all groups, one can give the exact value of  $n$ .

To obtain the exact values of the quantum numbers, one must use the technique. This technique is based on the fact that the groups of lines are precisely because of the Coriolis interaction. Figure 19 gives such a scheme for connecting points corresponding to the dependence of the intensities of the groups of lines upon the quantum numbers  $J$  and  $K_a$ . An example of the investigated and group assignments is shown in Fig. 20.

nearly 1 THz is com-  
ular rotational spectra  
rds were obtained only  
siderably lower sensit-  
quency measurements.  
ous spectra by microw-  
lysis of spectra. In this  
technique [34] (typical  
as well as the method

problem of searching for  
the initial model of the  
planation of the residual  
tained after the elimination  
is problem arose after  
COOH spectrum records  
molecule as an asymme-  
isplay of these groups of  
re each  $R_z$ -group of the  
these groups are 20–30  
of the ground state, which  
of vibrational satellites  
m of these groups of lines  
groups, which makes their  
of these groups relative to  
ting confirms the fact that  
OH molecule. The record  
t the corresponding places  
er, more similar to the  
so correspond to  $v_7 = 1$  or  
vibration (the out-of-plane  
between HCOOH and  
nd  $v_7 = 1$  in HCOOH are  
respectively [37]).

igated belong to the rota-  
l states  $v_7 = 1$  and  $v_9 = 1$   
hat as a result the order of  
go further, one must define

$v_7 = 1$  and  $v_9 = 1$  was pointed out

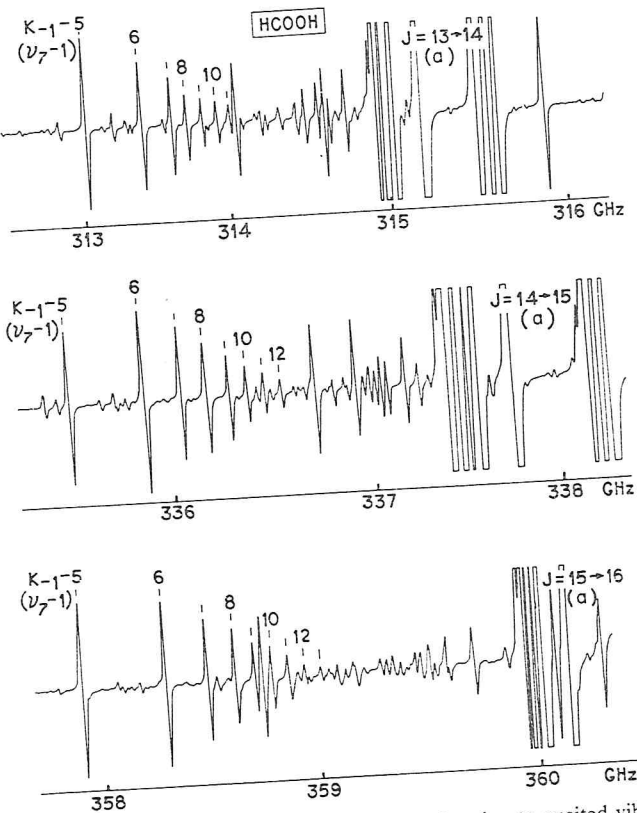


FIG. 18. Groups of lines in the HCOOH spectrum belonging to excited vibrational states. On the right the quantum numbers  $J$  of the transitions are indicated (large lines on the right belong to the ground vibrational state of HCOOH). On the left for the lines of the excited state  $v_7 = 1$ , the quantum numbers  $K_a$  are given.

The close relation of each group with an  $R_z$ -group of the ground state establishes the value of the quantum number  $J$  for each group. Taking into account that the dependence of line intensity on the quantum number  $K_a$  must remain similar for the ground and excited states one may deduce that the  $K_a$ -ordering changes for the lines in the group. However, this does not give the exact value of  $K_a$  for each line.

To obtain the exact value of  $K_a$  for each line we use the diagram technique. This technique, typical for an infrared band, can be applied precisely because of the broadband properties of the experimental method. Figure 19 gives such a diagram, where from the equal slopes of curves connecting points corresponding to similar lines for different  $J$  (similar dependence on  $J$ ) and from the appearance of  $K$ -splittings in the groups investigated and ground state groups, one succeeds in obtaining the transition assignments shown in the figure. First, transitions are identified in the

## 2.2 NEW METHO

122

A. F. KRUPNOV AND A. V. BURENIN

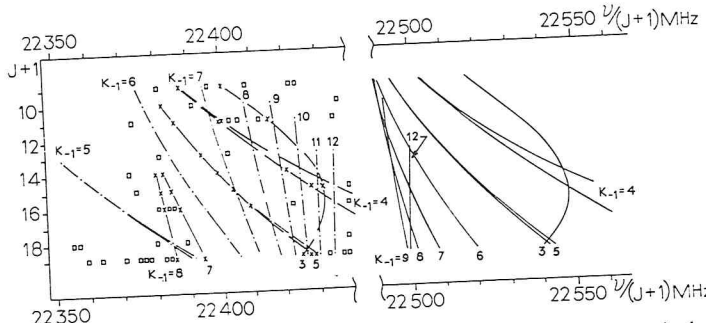


FIG. 19. The diagram used for assignment of rotational transitions in the excited vibrational states of the HCOOH molecule. Values of  $J + 1$  are plotted as ordinate, the experimental frequencies of transitions divided by  $J + 1$  are plotted as abscissa. Shown are branches with different  $K_a$  for the ground vibrational HCOOH state (—), for the excited vibrational state ( $v_7 = 1$ ) (— · —), and for the unidentified state (— × —) (by analogy according to the slope of the branch). The state  $v_7 = 1$  is strongly perturbed due to branches and the appearance of the  $K$ -splitting. The state  $v_9 = 1$  (the slope of the branch slightly changes, and the relative frequency ordering of the lines in the branch completely changes).

states  $v_7 = 1$  and  $v_9 = 1$  mentioned above. Then, after excluding the identified lines, more weak lines are accounted for, which do not undergo strong perturbations. Frequencies of 100 lines of the ground state, 50 lines of the state  $v_7 = 1$ , and 25 lines of the state  $v_9 = 1$  measured with an accuracy of  $10^{-6}$  in the submillimeter band permit one to establish the molecular parameters of HCOOH (the data will be published elsewhere).

Another interesting object of such "global" investigations of spectra may be rotational spectra in higher vibrational states excited by pumping one of the vibrational-rotational transitions with an infrared laser as in reference [39]. The general picture obtained for the change of rotational line intensities under the pumping action may yield valuable information about the laws of collisional excitation transfer. The high sensitivity of the method will make it possible to follow rather far the branches of the excitation transfer. Also of interest are microwave studies of vibrational-rotational molecular spectra for low frequency vibrations of pseudorotation, torsion, and bending types which fall within the submillimeter region.

### 4.3. NONLINEAR SPECTROSCOPY

The possibility of transmitting large radiation powers through the gas investigated in the RAD cell without increasing the receiver noise opens some new perspectives in nonlinear spectroscopy studies. The useful difference from existing methods lies here in the application of large radiation powers at any frequency including the frequency of the observed spectral

line. Large radiation fitting from the observed resonance" type of exchange" investigations.

(i) The observational molecules, the dipole moments presented there, such spectra by common situation in RAD em increasing the degree and with the increasing estimate the absorption molecules with a dipole to substitute the square

into the known expression

Here  $v_{\text{vib}}$  and  $\mu_{\text{vib}}$  moment matrix elements and excited vibration of molecules in the linewidth of the rotation differ from those for volume. Using Eqs. (we estimate the power signal-to-noise ratio

A. The polarization inducing the transition

$$(P_0/S) \sim (kT/8\pi)[(\Delta$$

B. The polarization field  $E_c$ .

$$(P_0/S) \sim [(kT)^2 \Delta]$$

2.2 NEW METHODS IN SUBMILLIMETER MICROWAVE SPECTROSCOPY 123

line. Large radiation fields could be applied earlier only at frequencies differing from the observed line frequency (to protect the detector). This "single resonance" type of experiment may now be added to such "double resonance" investigations. Some examples are given below.

(i) The observation of pure rotational spectra of completely nonpolar molecules, the dipole moment of which is induced by the electric field [40]. The existence of such transitions is mentioned in reference [2]. The estimations presented there, however, show the practical impossibility of observing such spectra by common microwave spectrometers. The improvement of the situation in RAD employing large power sources is associated both with increasing the degree of molecular polarization (i.e., spectral line intensity) and with the increase of RAD sensitivity at large radiation powers. To estimate the absorption coefficient of rotational transitions in nonpolar molecules with a dipole moment induced by the external field, it is necessary to substitute the square of the matrix element from reference [2]:

$$|d_{\text{eff}}|^2 \sim |\mu_{\text{vib}}|^4 E^2 / h^2 v_{\text{vib}}^2 \quad (27)$$

into the known expression for the absorption coefficient (at  $hv \ll kT$ )

$$\gamma \simeq (8\pi/3)(Nf/V)(v_{\text{rot}}^2 |d_{\text{eff}}|^2 / ckT \Delta\nu). \quad (28)$$

Here  $v_{\text{vib}}$  and  $|\mu_{\text{vib}}|$  are the frequency and the modulus of the dipole moment matrix element for the vibrational transition between the ground and excited vibrational states,  $E$  is the electric field strength,  $f$  is the fraction of molecules in the lower rotational state,  $v_{\text{rot}}$  and  $\Delta\nu$  are the frequency and linewidth of the rotational transition (the selection rules for this transition differ from those for ordinary electric dipole transitions [2]), and  $V$  is the cell volume. Using Eqs. (28) and (4), where  $\gamma l P_0$  is taken as the expression for  $P_s$ , we estimate the power flux necessary to observe the spectral line with a signal-to-noise ratio  $\sim 1$ . Two cases may be considered.

A. The polarization of the molecule is produced by the radiation field inducing the transitions.

$$(P_0/S) \sim (kT/8\pi)[(\Delta\nu)^2 \Delta\omega^{\text{cell}} \Delta\omega^{\text{rec}}/N]^{1/4} (v_{\text{vib}}/v_{\text{rot}}) \times (hc/|\mu_{\text{vib}}|^2)(1/f^{1/2}) \quad (29)$$

B. The polarization of the molecule is produced by an external constant field  $E_c$ .

$$(P_0/S) \sim [(kT)^2 \Delta\nu/8\pi](\Delta\omega^{\text{cell}} \Delta\omega^{\text{rec}}/N)^{1/2} (1/E_c^2) \times (v_{\text{vib}}^2 h^2 c/v_{\text{rot}}^2 |\mu_{\text{vib}}|^4)(1/f) \quad (30)$$

550 ν(J+1)MHz

λ<sub>k<sub>1</sub>=4</sub>

550 ν(J+1)MHz

in the excited vibrational coordinate, the experimental Shown are branches with excited vibrational state according to the slope of strongly perturbed due to slightly changes, and the angles).

after excluding the which do not undergo ground state, 50 lines of red with an accuracy establish the molecular elsewhere).

gations of spectra may ed by pumping one of d laser as in reference tational line intensities ation about the laws of he method will make it tation transfer. Also of onal molecular spectra ion, and bending types

owers through the gas ie receiver noise opens udies. The useful differentiation of large radiation of the observed spectral

Let us consider the numerical estimates. When  $N \sim 10^{17}$ ,  $T \sim 300^\circ\text{K}$ ,  $\mu_{\text{vib}} \sim 1 \text{ D}$ ,  $\Delta\omega^{\text{cell}} \sim 10^3 \text{ sec}^{-1}$ ,  $\Delta\omega^{\text{rec}} \sim 1 \text{ sec}^{-1}$ ,  $f \sim 10^{-2}$ ,  $E_c \sim 1 \text{ kV/cm}$ , and  $v_{\text{vib}}/v_{\text{rot}} \sim 10^2$ , which are all close to real figures, we obtain

$$(P_0/S) \sim \begin{cases} 10 \text{ W/cm}^2 & (\text{case A}) \\ 0.1 \text{ W/cm}^2 & (\text{case B}) \end{cases} \quad (31)$$

In the best experiments the true sensitivity of the RAD is now only 1.5 times lower than the limiting one. Thus, the estimates of the power flux should be increased by  $1.5^{1/2}$  times for case A and 1.5 times for case B, i.e., for  $S \sim 1 \text{ cm}^2$  the powers needed are near 12 and 0.15 W, respectively. These power levels are considerably lower than those already used in the RAD (see Section 2.5).

The observation of rotational spectra of nonpolar molecules is of interest since it permits the investigation of molecular polarization effects, and extends the class of molecules which may be investigated by microwave methods.

(ii) The direct observation of two-quantum absorption enables one to obtain narrow spectral lines, since the Doppler effect is compensated when a molecule absorbs two photons from waves traveling in opposite directions [41]. Again an object of interest may be completely nonpolar molecules (in case A when the polarization is produced by the radiation field itself).

### Conclusion

New methods have extended considerably the possibilities of microwave submillimeter spectroscopic investigations. In the submillimeter wave region, which corresponds to the highest attainable microwave frequencies, the molecular rotational spectrum intensity is maximum, i.e., there are optimal conditions for observing rotational spectra. A good combination of high sensitivity and resolving power, inherent to microwave methods, and broadband properties which were earlier achieved only by infrared methods provides a wealth of information and makes the methods described here rather promising. It may be expected that submillimeter studies will achieve a prominent place in molecular spectroscopy.

### ACKNOWLEDGMENTS

The authors are grateful to Academician A. V. Gaponov for his interest in the work and valuable discussions, to B. A. Andreev, S. P. Belov, A. N. Val'dov, L. I. Gershtein, V. P. Kazakov, E. N. Karyakin for assistance in preparing the manuscript. The authors are indebted to Dr. J. T. Hougen for reading the Russian-English translation and for making many valuable suggestions for improving the clarity of the English version of the manuscript, and to Dr. R. Pearson, Jr. for critical reading of the final text. Thanks are also due to Professor K. Narahari Rao for his time and effort.

The Soviet journals cite

- Izvestiya Vysshich Uchebnykh Zavedenii  
Electronics.  
Optika i Spektroskopiya—  
Pribory i Tekhnika Eksperimenta  
Radiotekhnika i Elektronika  
Zhurnal Eksperimental'noi  
Physics.
1. W. Gordy, W. V. Smith, *Millimeter Waves*, McGraw-Hill, New York, 1953.
  2. C. H. Townes and A. L. Schawlow, *Principles of Quantum Electronics*, McGraw-Hill, New York, 1955.
  3. W. Gordy, *Millimeter Waves*, Polytechnic Press of the University of Illinois, Urbana, 11, 403, (1965).
  4. W. Gordy and R. L. Johnson, *Millimeter Waves*, McGraw-Hill, New York, 1970.
  5. A. F. Krupnov, L. I. Gershtein, *Radiofiz. 13*, 1403 (1970).
  6. A. F. Krupnov, *Int. J. Quantum Electron.* 1, 1, 1972.
  7. A. F. Krupnov, *Colloq. Intern. C. P. 1973*.
  8. A. F. Krupnov, *Int. J. Quantum Electron.* 1, 1, 1974.
  9. S. P. Belov, A. V. Burenin, *Radiofiz. 16*, 295 (1971).
  10. A. V. Burenin and A. F. Krupnov, *Int. J. Quantum Electron.* 1, 1, 1972.
  11. "Quantum Electronic Spectroscopy," Sov. Radiotekhnika, No. 1, 1972.
  12. J. Tyndall, *Nature (London)*, 18, 19, 1972.
  13. M. B. Golant et al., *Int. J. Quantum Electron.* 1, 1, 1972.
  14. M. B. Golant et al., *Int. J. Quantum Electron.* 1, 1, 1972.
  15. A. V. Burenin, *Izv. Vuz. Radiofizika*, 16, 1, 1973.
  16. H. W. Harrington, *Int. J. Quantum Electron.* 1, 1, 1972.
  17. A. F. Krupnov and I. I. Antakarov, *Int. J. Quantum Electron.* 1, 1, 1972.
  18. S. P. Belov, A. V. Burenin, *Lett. Zh. Eksperim. i Teor. Fiz.* 16, 1, 1973.
  19. S. P. Belov, L. I. Gershtein, *Int. J. Quantum Electron.* 1, 1, 1973.
  20. L. O. Hocker, A. Javorka, *Int. J. Quantum Electron.* 1, 1, 1967.
  21. A. F. Krupnov and I. I. Antakarov, *Int. J. Quantum Electron.* 1, 1, 1972.
  22. A. N. Val'dov, L. I. Gershtein, *Int. J. Quantum Electron.* 1, 1, 1972.
  23. B. A. Andreev, S. P. Belov, *Int. J. Quantum Electron.* 1, 1, 1972.
  24. I. I. Antakarov, S. P. Belov, *Int. J. Quantum Electron.* 1, 1, 1972.

$\sim 10^{17}$ ,  $T \sim 300^\circ\text{K}$ ,  
 $0^{-2}$ ,  $E_c \sim 1 \text{ kV/cm}$ ,  
 we obtain

(31)

is now only 1.5 times power flux should be for case B, i.e., for  $I_1$ , respectively. These used in the RAD (see

molecules is of interest ionization effects, and ignited by microwave

option enables one to compensated when a in opposite directions onpolar molecules (in lation field itself).

sibilities of microwave submillimeter wave microwave frequencies, um, i.e., there are opti combination of high e methods, and broad infrared methods pro s described here rather studies will achieve a

his interest in the work and L. I. Gershtein, V. P. Kaza. The authors are indebted to d for making many valuable ie manuscript, and to Dr. R. due to Professor K. Narahari

#### References

- The Soviet journals cited in this article exist in English translation as follows:
- Izvestiya Vysshich Uchebnich Zavedenii, Radiofizika—Radiophysics and Quantum Electronics.
- Optika i Spektroskopiya—Optics and Spectroscopy.
- Pribory i Tekhnika Eksperimenta—Instruments and Experimental Techniques.
- Radiotekhnika i Elektronika—Radio Engineering and Electronics Physics.
- Zhurnal Eksperimental'noi i Teoreticheskoi Fiziki—Journal of Experimental and Theoretical Physics.
1. W. Gordy, W. V. Smith, and R. F. Trambarulo, "Microwave Spectroscopy." Wiley, New York, 1953.
  2. C. H. Townes and A. L. Schawlow, "Microwave Spectroscopy." McGraw-Hill, New York, 1955.
  3. W. Gordy. Millimeter and submillimeter waves in physics, *Proc. Symp. Millimeter Waves* Polytechnic Press of the Polytechnic Inst. of Brooklyn, New York, 1960; *Pure Appl. Chem.* **11**, 403, (1965).
  4. W. Gordy and R. L. Cook, "Microwave Molecular Spectra." Wiley (Interscience), New York, 1970.
  5. A. F. Krupnov, L. I. Gershtein, V. G. Shustrov and S. P. Belov, *Izv. Vyssh. Uchebn. Zaved. Radiofiz.* **13**, 1403 (1970).
  6. A. F. Krupnov, *Int. Seminar High Resolution IR Spectrosc.*, 2nd Abstracts of papers, Prague (1972).
  7. A. F. Krupnov, *Colloq. High Resolution Mol. Spectrosc.*, 3rd Abstracts of papers, Tours (1973).
  8. A. F. Krupnov, *Int. Seminar High Resolution IR Spectrosc.*, 3rd Abstracts of papers, Prague (1974).
  9. S. P. Belov, A. V. Burenin, L. I. Gershtein, V. V. Koroliukin, and A. F. Krupnov, *Opt. Spektrosk.* **35**, 295 (1973).
  10. A. V. Burenin and A. F. Krupnov, *Izv. Vyssh. Uchebn. Zaved. Radiofiz.* **17**, 1242 (1974).
  11. "Quantum Electronics." Sov. Encyclopaedia, Moscow (1969).
  12. J. Tyndall, *Nature (London)* **23**, 374 (1880–1881); W. G. Röntgen, *Wied Ann.* **12**, 153, (1881).
  13. M. B. Golant et al., *Prib. Tekh. Eksp.* **4**, 136 (1965).
  14. M. B. Golant et al., *Prib. Tekh. Eksp.* **3**, 231 (1969).
  15. A. V. Burenin. *Izv. Vyssh. Uchebn. Zaved. Radiofiz.* **17**, 1291 (1974).
  16. H. W. Harrington, I. R. Hearn, and R. F. Rauskolb, *Hewlett-Packard J.* **22**, 10, 2 (1971).
  17. A. F. Krupnov and L. I. Gershtein, *Prib. Tekh. Eksp.* **6**, 143 (1970).
  18. S. P. Belov, A. V. Burenin, L. I. Gershtein, V. P. Kasakov, E. N. Karyakin, and A. F. Krupnov, *Lett. Zh. Eksp. Teor. Fiz.* **18**, 285 (1973).
  19. S. P. Belov, L. I. Gershtein, E. N. Karyakin, and A. F. Krupnov, *Prib. Tekh. Eksp.* **3**, 142 (1973).
  20. L. O. Hocker, A. Javan, D. Ramachandra Rao, L. Frenkel, and T. Sullivan, *Appl. Phys. Lett.* **10**, 147 (1967).
  21. A. F. Krupnov and L. I. Gershtein, *Prib. Tekh. Eksp.* **5**, 130 (1970).
  22. A. N. Val'dov, L. I. Gershtein, E. N. Karyakin, A. F. Krupnov, and A. V. Maslovsky, *Prib. Tekh. Eksp.* **5**, 110 (1974).
  23. B. A. Andreev, S. P. Belov, A. V. Burenin, L. I. Gershtein, and A. F. Krupnov, *Radiotekh. Elektron.* **19**, 1318 (1974).
  24. I. I. Antakov, S. P. Belov, L. I. Gershtein, V. A. Gintzburg, A. F. Krupnov, and G. S. Parshin, *Lett. Zh. Eksp. Teor. Fiz.* **19**, 634 (1974).

25. A. V. Gaponov, M. I. Petelin, and V. K. Yulpatov, *Izv. Vyssh. Uchebn. Zaved. Radiofiz.* **10**, 1414 (1967).
  26. T. A. DeTemple, T. K. Plant, and P. D. Coleman, *Appl. Phys. Lett.* **22**, 614 (1973).
  27. M. Mizushima and P. Venkateswarlu, *J. Chem. Phys.* **21**, 705 (1953); I. M. Mills, J. K. G. Watson, and W. L. Smith, *J. Mol. Phys.* **16**, 329 (1969).
  28. J. K. G. Watson, *J. Mol. Spectrosc.* **40**, 536 (1971); K. Fox, *Phys. Rev. Lett.* **27**, 233 (1971).
  29. F. Y. Chu and T. Oka, *J. Chem. Phys.* **60**, 4612 (1974).
  30. J. K. G. Watson, *J. Chem. Phys.* **46**, 1935 (1967).
  31. Yu. V. Linnik, Least squares method and the basis of mathematico-statistical theory of the data processing, Fizmatgiz, Moscow (1962).
  32. M. I. Ageev (ed.), "General questions of programming," in "Algorithms." VTz. AS USSR, 1966.
  33. A. V. Burenin, A. F. Krupnov, and A. B. Yagnetinsky, *Izv. Vyssh. Uchebn. Zaved. Radiofiz.* **17**, 1136 (1974).
  34. T. Nakagawa and J. Overend, *J. Mol. Spectrosc.* **50**, 333 (1974).
  - 34a. J. F. Scott and K. Narahari Rao, *J. Mol. Spectrosc.* **20**, 461 (1966).
  - 34b. S. Ghergetti and K. Narahari Rao, *J. Mol. Spectrosc.* **28**, 27 (1968).
  - 34c. A. W. Mantz and K. Narahari Rao, *J. Mol. Spectrosc.* **30**, 513 (1969).
  - 34d. K. Narahari Rao, *Annal. N.Y. Acad. Sci.* **220**, 17 (1973).
  35. R. Pearson, T. Sullivan, and L. Frenkel, *J. Mol. Spectrosc.* **34**, 440 (1970).
  36. J. K. G. Watson, *J. Mol. Spectrosc.* **50**, 281 (1974).
  37. L. M. Sverdlov, M. A. Kovner, and E. P. Krainov, "Vibrational Spectra of Molecules." Fizmatgiz, Moscow, 1970.
  38. C. Samson, J. Bellet, E. Willemot, and G. Steenbeckeliers, *Bull. Acad. Roy. Belg. Ser. 5* **9**, 921 (1970).
  39. T. Y. Chang, T. J. Bridges, and E. G. Burkhardt, *Appl. Phys. Lett.* **17**, 249 (1970).
  40. A. V. Burenin and A. F. Krupnov, *Zh. Eksp. Teor. Fiz.* **67**, 510 (1974).
  41. L. S. Vasilenko, V. P. Chebotaev, and N. V. Shishaev, *Lett. Zh. Eksp. Teor. Fiz.* **12**, 161 (1970).

Labs

## 1. Introduction

Renner's classic problem of E. Teller's, appeared in its infancy. It was reported, in the specification that Renner had not had treated only linear molecules NCO [16]. Renner's ideas more clearly describe the coupling around the axis of a molecule. It includes molecules that are not just a spectrum. The definition of family complexity of the

† On leave (1974-19  
Vancouver, British Co